

A new dinosaur (Saurischia: Sauropodomorpha) from the Late Triassic of Brazil provides insights on the evolution of sauropodomorph body plan

FLÁVIO A. PRETTO^{1,2,*}, MAX C. LANGER³ AND CESAR L. SCHULTZ²

¹*Centro de Apoio à Pesquisa Paleontológica da Quarta Colônia, Universidade Federal de Santa Maria, Rua Maximiliano Vizzotto 598, 97230-000 São João do Polêsine, Rio Grande do Sul, Brazil*

²*Programa de Pós-Graduação em Geociências, Universidade Federal do Rio Grande do Sul, Av. Bento Gonçalves 9500, 91540-000 Porto Alegre, Rio Grande do Sul, Brazil*

³*Laboratório de Paleontologia de Ribeirão Preto, FFCLRP, Universidade de São Paulo, Av. Bandeirantes 3900, 14040-901 Ribeirão Preto, São Paulo, Brazil*

Received 2 July 2017; revised 11 March 2018; accepted for publication 4 April 2018

A new sauropodomorph dinosaur from the Late Triassic Candelária Sequence (Santa Maria Formation), south Brazil, *Bagualosaurus agudoensis* gen. et sp. nov., helps to fill a morphological gap between the previously known Carnian members of the group and younger sauropodomorphs. In some aspects, the skull, lower jaw, and dental anatomy of the new taxon approaches that seen in Norian forms like *Pantyraco caducus*, *Efraasia minor*, and *Plateosaurus engelhardti*. On the contrary, the post-cranial skeleton is broadly reminiscent of coeval, early dinosaurs. Although not reaching the size of most Norian and younger sauropodomorphs, *B. agudoensis* is significantly larger than coeval forms. The new data thus suggest that modifications in skull anatomy, possibly related to more efficient herbivorous habits, appeared early in sauropodomorph evolution, along with a moderate increase in size, followed in post-Carnian times by further increase in size, accompanied by more radical changes in post-cranial anatomy.

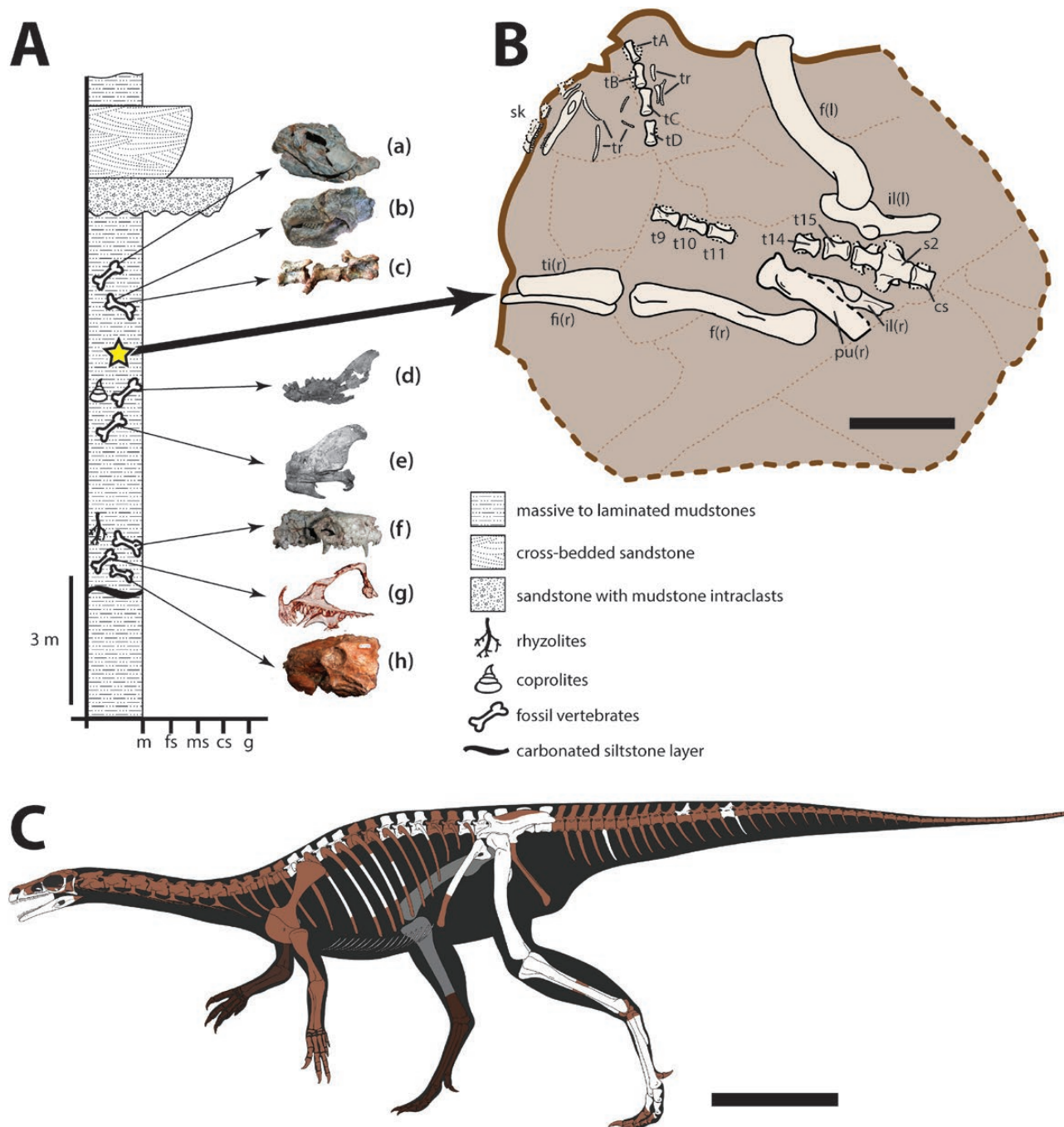
ADDITIONAL KEYWORDS: Candelária Sequence – Early dinosaurs – Late Triassic – Santa Maria Formation – Sauropodomorpha.

INTRODUCTION

Sauropodomorphs are an iconic component of Mesozoic faunas, with some representatives (grouped within Sauropoda) achieving the largest body sizes ever recorded among land vertebrates (Sander & Clauss, 2008; Sander *et al.*, 2011). The oldest sauropodomorphs are from the Late Triassic (Carnian) (Langer *et al.*, 1999; Martínez & Alcober, 2009; Ezcurra, 2010; Cabreira *et al.*, 2011; Sereno, Martínez & Alcober, 2013; but see: Baron *et al.*, 2017a), a time when the group experienced a rapid increase in diversity, becoming the most diverse Triassic dinosaurian clade (Irmis, 2011). Nonetheless, during the pre-Norian stages of

their evolution, sauropodomorphs (as well as other dinosaur groups) were relatively rare in the fossil record. Carnian sauropodomorphs come from deposits of the Candelária Sequence (Santa Maria Formation) in southern Brazil and include *Saturnalia tupiniquim*, *Pampadromaeus barberenai* and *Buriolestes schultzi* (Langer *et al.*, 1999; Cabreira *et al.*, 2011, 2016); and from the Ischigualasto Formation of north-western Argentina, with *Eoraptor lunensis*, *Panphagia protos* and *Chromogisaurus novasi* (Sereno *et al.*, 1993, 2013; Martínez & Alcober, 2009; Ezcurra, 2010). In both geological units, the group is a minor component of vertebrate faunas, and is represented by taxa of relatively modest body size (Martínez *et al.*, 2013; Sereno *et al.*, 2013; Pretto, Schultz & Langer, 2015). Apart from the size, these sauropodomorphs lack many anatomical traits shared by post-Carnian members of the group (e.g. teeth with large denticles, robust hindlimbs and fully perforated acetabulum),

*Corresponding author. E-mail: flavio.pretto@ufsm.br
[Version of Record, published online 25 May 2018;
<http://zoobank.org/urn:lsid:zoobank.org:pub:D848571F-5EE7-47AD-82BB-B20106BD1549>]



rather displaying a mosaic of plesiomorphic features and even putative theropod characteristics (Cabreira *et al.*, 2011, 2016; Sereno *et al.*, 2013; Langer, 2014).

Here we present the remains of a new sauropodomorph from the Late Triassic of southern Brazil. The specimen, apart from possessing a combination of characters distinct from those of coeval Carnian dinosaurs, shows several traits, mostly of the skull and dentition, known until now only in Norian (or younger) sauropodomorphs. The new specimen not

only increases known sauropodomorph diversity during the first stages of dinosaur evolution, but partially fills a morphological gap between the earliest sauropodomorphs and the Norian members of the group. The recognition of a new sauropodomorph adds to the diversity of the group in Late Triassic times, agreeing with the idea that, prior to their ecological dominance, the group experienced a period of low abundance and high diversification (Ezcurra, 2010; Irmis, 2011).

INSTITUTIONAL ABBREVIATIONS

MCN-PV, vertebrate paleontology collection at Museu de Ciências Naturais, Fundação Zoobotânica do Rio Grande do Sul, Brazil; ULBRA-PVT, vertebrate paleontology collection at Universidade Luterana do Brasil, Canoas, Brazil; UFRGS-PV, vertebrate paleontology collection at Universidade Federal do Rio Grande do Sul, Brazil.

GEOLOGICAL SETTINGS

The holotype material of the new taxon (see below) was found at the Janner outcrop, about 2 km from the town of Agudo, Rio Grande do Sul, Brazil. The lithology of the site (Fig. 1A) comprises massive red beds, including siltstones and very thin sandstones, that locally incorporate mud inclusions and sporadic rhythmic mudstone–siltstone intervals. These strata are interpreted as representative of a distal floodplain accumulation, and a cross-bedded sandstone preserved at the top of the exposure represents a river channel. An important set of vertebrate fossils has been already collected from the site. These include the type-materials of the early sauropodomorph *Pampadromaeus barberenai* (Cabreira *et al.*, 2011) and the carnivorous cynodont *Trucidocynodon riograndensis* (de Oliveira, Soares & Schultz, 2010). The predominant taxon at the site is the herbivorous traversodontid *Exaeretodon riograndensis*, but rhynchosaurs (Hyperodapedontidae) and non-identified dinosauromorph remains have also been reported from the site (de Oliveira *et al.*, 2007; Liparini *et al.*, 2013; Müller *et al.*, 2014; Pretto *et al.*, 2015).

The presence of hyperodapedontid rhynchosaurs (*Hyperodapedon* sp.), together with *Exaeretodon riograndensis*, allows a biostratigraphic correlation of the Janner site with the *Hyperodapedon* Assemblage Zone, part of the Candelária Sequence of the Santa Maria Formation (Abdala, Ribeiro & Schultz, 2001; Horn *et al.*, 2014). The *Hyperodapedon* Assemblage Zone correlates with the late Carnian deposits of the Ischigualasto Formation in

Argentina (Langer, 2005; Martínez *et al.*, 2013), which provided radiometric dates (Rogers *et al.*, 1993; Martínez *et al.*, 2011). Recent U-Pb zircon geochronology data on the levels referable to the *Hyperodapedon* Assemblage Zone provided a c. 233 Mya age for those levels (Langer, Ramezani & Da Rosa, 2018). Interestingly, the upper portion of that unit also shows a prevalence of *Exaeretodon* (Cabrera, 1943; Martínez *et al.*, 2013), following a decline in hyperodapedontid rhynchosaur (*Scaphonyx sanjuanensis*) abundance, suggesting that it might be directly correlated with the Janner outcrop (Langer, 2005; Liparini *et al.*, 2013; Pretto *et al.*, 2015).

SYSTEMATIC PALEONTOLOGY

DINOSAURIA OWEN, 1842 *SENSU* PADIAN & MAY, 1993

SAURISCHIA SEELEY, 1887 *SENSU* GAUTHIER, 1986

SAUROPODOMORPHA VON HUENE, 1932

BAGUALOSAURUS AGUDOENSIS GEN. ET SP. NOV.

Holotype

UFRGS-PV-1099-T, a semi-articulated skeleton, including partial skull and mandible, trunk vertebrae, sacrum and isolated caudal vertebrae, fragmented ribs, gastralia, isolated haemal arches, both ilia, right pubis, femora, tibiae, fibulae and partial left pes (Fig. 1B, C).

Etymology

The generic name is derived from the term ‘Bagual’, a term employed regionally in southern Brazil to refer to an animal or person of strong build or valour, plus ‘saurus’, Latin, meaning lizard; the specific name makes allusion to the town of Agudo, where the holotype was collected.

Type locality and horizon

Reddish mudstone at the mid-portion of the strata exposed at the Janner site (53°17′34.20″ W, 29° 39′ 10.89″ S), Agudo municipality, Candelária Sequence, Santa Maria Supersequence (Horn *et al.*, 2014).

Figure 1. A, Stratigraphic section of the Janner outcrop (Candelária Sequence, Late Triassic, Brazil), with the position of selected specimens (specimen photographs not to scale). (a) *Hyperodapedon* sp., MCN-PV-3509; (b, d, e) *Exaeretodon riograndensis*, respectively UFRGS-PV-0715-T, 1096-T and 1177-T; (c) *Dinosauria* indet., UFRGS-PV-1240-T; (f) *Trucidocynodon riograndensis*, UFRGS-PV-1051-T; (g) *Pampadromaeus barberenai*, ULBRA-PVT-016; (h) juvenile traversodontid (possibly *E. riograndensis*), UFRGS-PV-1160-T. Star indicated the provenance of the holotype of *Bagualosaurus agudoensis*. B, Schematic drawing of UFRGS-PV-1099-T, as originally preserved. Left tibia, fibula and foot were displaced from their original position prior to collection and are not shown, as well as several unidentified fragments. Information on the exact location of the gastralia, caudal vertebrae and haemal arches within the matrix block was not recovered. Solid brown line marks the original surface that exposed the specimen in the field; dashed brown line indicates the limits of the collected block. Abbreviations: cs, caudosacral; f, femur; fi, fibula; il, ilium; pu, pubis; s, sacral vertebra; sk, skull and lower jaw t, truncal vertebra; ti, tibia; tr, fragmented truncal ribs. Scalebar: 10 cm. C, Schematic drawing of *Bagualosaurus agudoensis*. Preserved elements indicated in white (grey for the right side). Missing elements represented in dark brown. The preserved right pubis is mirrored in the image. Scale bar: 20 cm.

Diagnosis

A gracile, medium-sized sauropodomorph with a unique combination of features, including (* = autapomorphies): a short skull, less than two-thirds of femoral length; premaxillary and dentary teeth retreated from the rostral margin of the snout; first premaxillary tooth at least as high as the highest tooth in the maxillary row; absence of a subnarial gap or diastema; most teeth lanceolate with coarse serrations along the carinae; ventral acetabular margin of the ilium straight; dorsal surface of the iliac acetabulum straight, with the supracetabular crest not overhanging the acetabulum ventrally*; lateromedially widened pubic peduncle, with no dorsal crest; pubic tubercle with a distinct longitudinal sulcus*; femoral length subequal to the length of tibia/fibula; absence of a marked fibular crest on tibia; distal tibia with a conspicuous caudomedial notch; gracile metatarsals. Additional diagnostic features are provided in the [Supporting Information](#).

Description

Taphonomic remarks: The holotype of *Bagualosaurus agudoensis* consists of a partial, semi-articulated skeleton (Fig. 1B). The material was collected from a small ravine, and some of its elements were eroded prior to discovery. This includes most of the skull roof and the distal part of the hindlimbs, some elements of which (e.g. left tibia, fibula and pes) were recovered close to the main block containing the articulated portions. The initial exposure of the specimen revealed that it was buried lying on its back, an unusual situation among archosaurs (Cambra-Moo & Buscalioni, 2003). The positioning of the hindlimbs is equally uncommon, as the legs were preserved extended parallel to the main trunk axis, with their distal portions facing cranially. The recovered vertebrae were preserved in three separate segments (two including vertebrae from the front and rear part of the trunk and a third one with the sacrum and neighbouring elements), but most ribs were disarticulated or fragmented. The ilia were preserved close to the sacrum, but slightly displaced cranially. The right pubis was also close to its original position. The skull and mandible remains were preserved in articulation, with various elements missing due to recent erosion. They were buried close to their expected original position (as suggested by the articulation of the skull and jaw elements), but there are no remains of cervical vertebrae nearby.

Most elements of the holotype show evidence of weathering. This is particularly clear in thin elements, like the neural spines of the vertebrae, which show a brittle, flaked surface. Indeed, most vertebrae have incomplete neural spines and transverse processes, and the matrix surrounding them was packed with small, bone splinters, still embedded in the sediment. The same is seen in the caudal portion of the

lower jaw. This evidence allows the specimen to be categorized somewhere between Weathering Stages 2 and 3 of Behrensmeyer (1978), suggesting long-term exposure prior to final burial. Most elements are significantly worn at the articular extremities, where cancellous bone was predominant. Several elements show evidence of osteophagic activity in these areas, possibly related to the action of insects or other invertebrates (Paes Neto *et al.*, 2016). Such alterations include tunnel excavation in the bones, etching and deep furrows along the bone surfaces. It is also possible that the loss of elements (e.g. forelimb), as well as the unusual position of the carcass as preserved, may be the result of the activity of vertebrate scavengers, but unequivocal evidence of tooth marks was not found. Some bones were also deformed by diagenetic processes, including compression (i.e. left femur), or a slight disruption of the bone surface caused by the early formation of calcite and its subsequent volumetric expansion during crystallization (Holz & Schultz, 1998). Calcite concretions are also common within bone cavities, and their hardness made preparation unfeasible in some portions where the bone was fragile.

Skull: The skull of *Bagualosaurus agudoensis* (Fig. 2) is slender and relatively short, less than two-thirds of the femoral length. As better seen in right lateral view, the orbit is large, with a preserved diameter about one-third of the total skull length. The antorbital fossa, although not fully preserved, seems to have a similar rostrocaudal length, as inferred based on both sides of the skull. Most of the dorsal elements of the skull were eroded prior to the discovery of the specimen, and the caudal portion of the skull is equally damaged. The right side is overall better preserved, but the following description reflects, unless otherwise mentioned, a general agreement between the information provided by both counterparts.

The premaxilla of *Bagualosaurus agudoensis* has a subrectangular body in lateral view, and a single neurovascular foramen pierces its rostral portion. This corresponds to the anterior premaxillary foramen (Sereni *et al.*, 2012), and is located dorsal to the first premaxillary tooth (right side), or between the first and second premaxillary teeth (left side). A very faint dorsal concavity marks the premaxillary contribution to the narial fossa, and the premaxillary foramen is located outside this depression. The rostradorsal process of the premaxilla is broken at its base, and the rostralmost portion of the external naris is positioned caudal to the mid-length of the premaxillary body. The caudodorsal process probably had a minor contribution to the caudal margin of the external naris. The caudal margin of the premaxillary body bears a distinct notch, with a similar counterpart in the cranial portion of the

maxilla, which together form the subnarial foramen. The premaxillary tooth row of *Bagualosaurus agudoensis* is caudally displaced, so that the bone has a rostral portion that lacks teeth, with a length equivalent to at least one tooth position.

The maxilla is incomplete in both sides of the skull, but the combined preserved counterparts encompass most of its anatomy. The rostral process of the bone articulates with the premaxilla, and contributes to the caudal margin of the subnarial foramen. There is no subnarial gap, nor diastema, and the tooth row is continuous between the premaxilla and maxilla. The maxillary rostral process is ventrorostrally tapering, with

a rounded rostral margin. The narial fossa does not excavate the lateral surface of the maxillary rostral process. At least three foramina perforate the lateral side of the left maxilla, their disposition resembling that of other sauropodomorphs (e.g. Sues *et al.*, 2004; Cabreira *et al.*, 2011; Prieto-Márquez and Norell, 2011; Sereno *et al.*, 2013). The right maxilla preserved the remains of the last foramen of the row, which is large and opens caudally, forming a shallow groove. The rostral portion of the antorbital fossa is formed by a recessed lamina of the ascending process of the maxilla, but most of both structures are missing. Two shallow oval pouches are seen within the antorbital fossa,

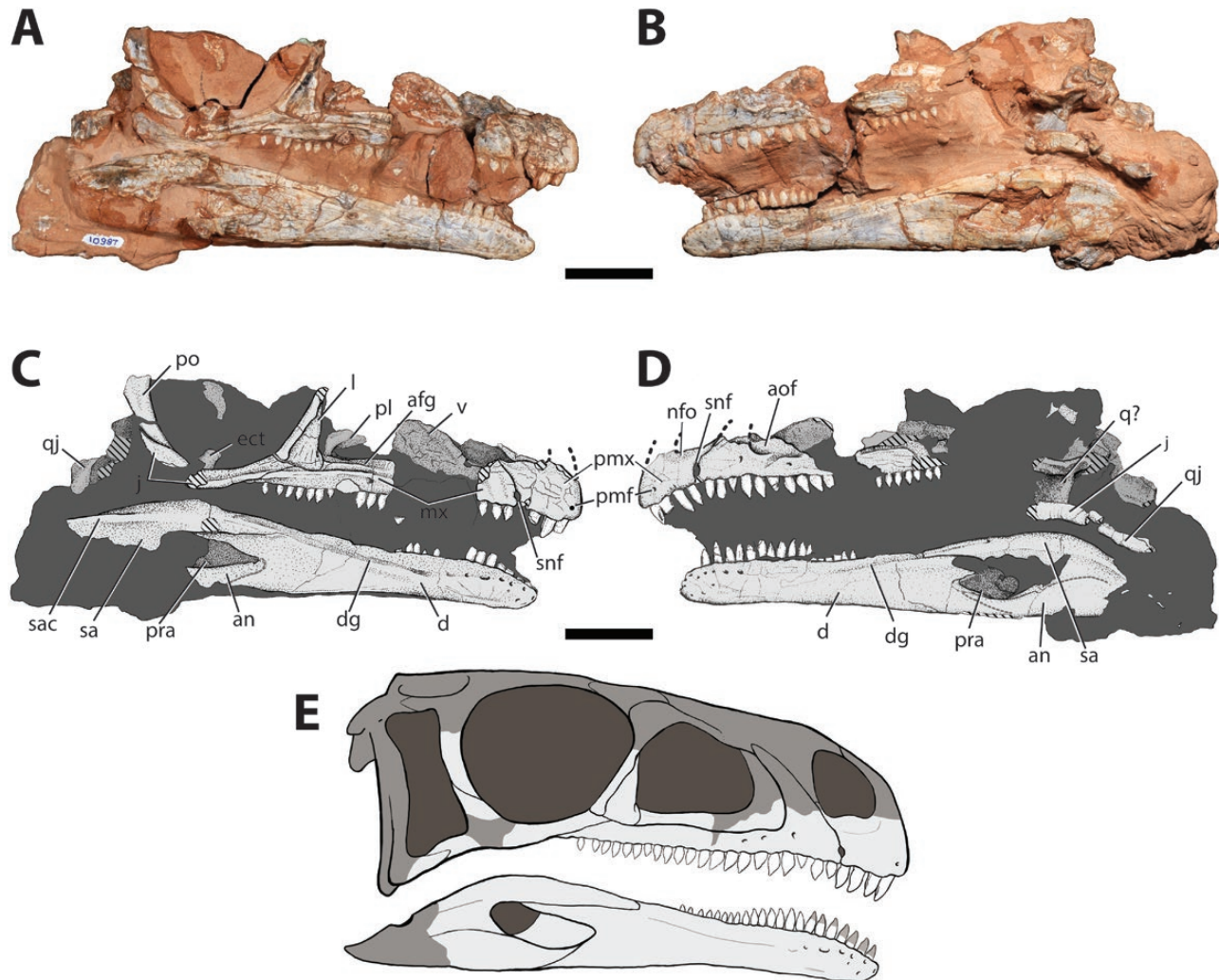


Figure 2. *Bagualosaurus agudoensis* (UFRGS-PV-1099-T), photographs and interpretive drawings of the skull and mandible in right lateral view (A, C), and left lateral view (B, D). Hatched surfaces indicate missing portions. Dashed lines show reconstructions of bone outline, and dark grey areas represent the sediment. Abbreviations: afg, groove at the floor of antorbital fossa; aof, antorbital fossa; an, angular; d, dentary; dg, dentary groove; ect, ectopterygoid; j, jugal; l, lacrimal; mx, maxilla; pl, palatine; pmf, premaxillary foramen; pmx, premaxilla; po, postorbital; pra, prearticular; q, quadrate; qj, quadratejugal; sa, surangular; sac, crest on surangular; snf, subnarial foramen; v, vomere. E, reconstruction of the skull in lateral view. Missing portions shown in grey. Scale bars: 2 cm.

but these are not perforating. The maxilla contributes to most of the ventral margin of the antorbital fossa and the ventral limit of the latter is marked by a sharp longitudinal crest that extends along the lateral surface of the maxillary caudal ramus. The floor of the antorbital fossa bears a marked groove, perforated by a dorsally opening neurovascular foramen. The caudal ramus of the maxilla is long and straight, with dorsal and ventral margins that are parallel for most of its length. The ramus tapers only in its caudalmost portion, where the maxilla is laterally overlapped by the jugal. The slender extremity of the caudal ramus of the maxilla extends ventral to that bone, and almost reaches the midpoint of the orbit, caudally.

Only the ventral ramus of the right lacrimal is preserved. It slopes rostrally as it extends dorsally, and its caudal margin forms the rostral margin of the orbit. It has a lateral excavation at its rostral margin, the caudal margin of which is slightly everted. It expands ventrally forming a triangular depression, which represents the caudoventral portion of the antorbital fossa. The ventral ramus of the lacrimal rests in a broad contact with the maxilla and jugal. In the caudal portion of this contact, the lacrimal overlaps the jugal and, rostral to that, the lacrimal rests in a trough of the maxilla, effectively isolating the jugal from the internal antorbital fenestra.

Parts of the rostral and dorsal processes of the right jugal are preserved. From the left jugal, only a fragment of the caudal process remained. The rostral process is slightly dorsally expanded at its tip, with an articular facet that is overlapped by the caudal portion of the ventral ramus of the lacrimal. The tip of the rostral process reaches the antorbital fossa, but not the internal antorbital fenestra. A marked crest, an extension of the longitudinal crest of the maxilla, extends along the lateroventral surface of the rostral process of the jugal. Ventral to that, a deep longitudinal excavation accommodates the caudal extremity of the maxilla, which laterally covers most of the ventral surface of the preserved rostral process of the jugal. The dorsal margin of the rostral process is concave, forming the ventral border of the orbit. On the contrary, the dorsal process is nearly excluded from the orbit by the postorbital. The lateral surface of the small fragment of the caudal process of the left jugal is apparently plain and featureless.

Only part of the ventral process of the right postorbital is preserved. In lateral view, its ventral portion is gently curved rostrally, where it contacts the dorsal process of the jugal. Its cranial margin is concave, and forms most of the caudal margin of the orbit.

Caudal to the orbits, the skull is badly preserved, with most of its elements missing. Indeed, the quadratojugal is preserved in both sides of the skull only as fragments. On the left side, it is disarticulated from the quadrate, a taphonomic condition commonly reported

for sauropodomorphs (Sereño *et al.*, 2013). The caudal portion of the bone is lateromedially expanded. Both the jugal and the quadratojugal project ventrally, fitting the caudodorsal outline of the surangular and suggesting that *Bagualosaurus agudoensis* had a ventrally deflected jaw joint.

The right palatine is fragmentary, but its rostradorsal flange and rostral process are exposed in lateral view through the right antorbital fenestra. Some fragments preserved medial to the caudal portion of the left maxilla may represent the left palatine, but their preservation hampers a clear identification. The most prominent feature preserved in the right palatine is the rostradorsal flange. Only the area surrounding its base was preserved, showing a rostradorsally bowed caudal ridge, and a slender lamina that projects further rostrally, but the complete extent of the palatine cannot be assessed. The slender rostral process projects from the base of the rostradorsal flange, and contacts the maxilla laterally.

Both vomera can be observed interposed between the maxillae. Their footplates are not exposed, but their dorsal laminae are clearly seen. They form two broad sheets of bone contacting one another medially. The dorsal lamina of the vomer is slightly sloped, and its craniodorsal rim is more robust than the rest of the lamina. The caudal portion of the vomera is badly preserved, and it is not possible to infer the presence of a caudal contact with the palatine.

Several preserved bone fragments might be related to palatal elements. At the right side of the skull, close to the midpoint of the ventral rim of the orbit, a small fragmentary portion of the right ectopterygoid can be observed. It contacts the medial surface of the jugal, but is probably displaced dorsally. On the left side, some fragments located mediodorsally to the caudal portion of the maxilla might represent displaced parts of the pterygoid, but they are too poorly preserved to allow the identification of any anatomical features. An element exposed in the left side of the skull is putatively identified as the left quadrate. Interpreted as such, this element is displaced from its original position, and rotated almost 180 degrees, with its medial surface facing laterally and the ventral portion facing dorsally. Its craniodorsal tip is not exposed, but the caudal margin of the element is rostrally bowed, and the inferred condyle area is obscured by additional fragmentary elements of indeterminate identity.

Mandible: Both hemimandibles are preserved in articulation, but the articulation with the skull is missing. The mandibles are exposed in lateral view. Assuming they are in their natural position, the rostral tip of the dentary is ventral to the space between the first and second premaxillary teeth. As a whole, the mandible is slender, rostrocaudally elongated and

dorsoventrally low, probably with a ventrally deflected articular region, as inferred from the curvature seen in the surangular.

The dentary is the longest mandibular element, exceeding half the total inferred length of the lower jaw. Its rostral portion is perforated by several foramina, most of them aligned near the dorsal surface of the bone, and opening either dorsally or rostrally. A longitudinal groove starts caudal to this line of foramina and extends along the entire length of the bone, ventral to its dorsal margin. The rostral tip of the dentary is rounded and its dorsal margin is slightly sloped ventrally. As in the premaxilla, it also lacks teeth, as the tooth row is caudally displaced one tooth position away from the rostral edge of the bone. The ventral margin of the dentary is slightly concave in lateral view, but the dorsal margin is straight. Caudally, the dentary is forked into dorsal and ventral processes. The ventral surface of the former forms the rostradorsal margin of the mandibular fenestra, and its dorsal surface is overlapped by the surangular. The ventral process seems to be shorter, but its limits are difficult to define. It is inferred to overlap the angular and not to contribute to the mandibular fenestra.

The surangular is preserved in both hemimandibles, but its caudal tip, including the area of the retroarticular process, is missing. The bone overlaps the caudodorsal margin of the dentary and possesses a long rostral process that fits in the dorsal dentary groove. This portion of the surangular also shows a slight longitudinal groove that ends close to the midpoint of the mandibular fenestra. At this point, the surangular is perforated by a foramen that opens rostrolaterally. Ventral to the surangular groove and extending along the entire preserved portion of the bone, a conspicuous longitudinal crest is seen, which is more prominent caudally. The rostral, fainter portion of this crest is better seen in the left bone, whereas its caudal, sharpest portion is more evident in the right side. The dorsal margin of the surangular is convex and its caudal portion is ventrally deflected. The surangular contributes to the caudodorsal and caudal margins of the mandibular fenestra, and contacts the angular ventrally.

The angular is an arched element, with a dorsally concave margin that forms the ventral border of the mandibular fenestra. It is preserved in both hemimandibles, but the right element lacks its entire caudal portion. The bone is overlapped rostrally by the dentary and contacts the surangular at its caudodorsal portion, where it is excluded from the caudal margin of the mandibular fenestra.

The lateral surface of the prearticular is partially exposed in both hemimandibles through the mandibular fenestra, but little can be said about their morphology.

Dentition: The tooth rows are incomplete both in the upper and lower jaws. There are four premaxillary teeth and at least 23 maxillary teeth, as inferred from the preserved portions of both sides. The more complete left dentary tooth row has 18 preserved teeth, but this does not represent the full series. The presence of palatal teeth is uncertain. As already stated, the first premaxillary tooth is inset from the rostral margin of the premaxilla. Although broken at their bases, the rostralmost dentary teeth of *Bagualosaurus agudoensis* are also clearly inset from the rostral tip of the dentary. The last preserved maxillary tooth is located below the orbit. The upper tooth row seems continuous along the premaxilla and maxilla, with no evidence of a diastema. At least two teeth (the 3rd and 6th maxillary teeth) show signs of replacement, given their shorter crowns and sharper denticles.

Most teeth show a slight caudal curvature, including the last teeth in the upper and lower rows. All teeth show some lateral expansion, more evident in the bulbous teeth of the caudal part of the maxillae. Additionally, all teeth bear a basal constriction, as to achieve a lanceolate crown shape. This constriction is not evident in newly erupting teeth, because it is hidden by the alveolar margin, and seems to be less marked in the rostralmost preserved teeth, both in the premaxillae and the dentaries.

The denticles are generally large, with a density of 3–5 denticles per millimeter. They are obliquely set relative to the crown margin, and those in the mesial carina seem larger than those in the distal one. The denticles apparently extend further towards the crown base in the distal carina, whilst the denticles of the mesial carina are usually restricted to its apical third. The denticles are commonly worn away in the mesial carina of older teeth. There is also no evidence of denticles in the premaxillary teeth and the rostralmost dentary elements. The reason for this absence, whether due to anatomy, tooth wear or taphonomy, is uncertain.

The premaxillary teeth are less lanceolate than other teeth in the upper row. The ventral alveolar margin of the premaxilla is almost straight, only slightly sloped ventrally towards the tip. The first premaxillary tooth is as high as any of the maxillary tooth crowns, but the second and third premaxillary teeth are slightly higher.

Among the maxillary teeth, the fourth and fifth teeth are the highest in the series. Caudal to those, the tooth crowns progressively reduce in height. Some maxillary tooth crowns show signs of wearing, identified by the partial absence of denticles in the mesial carina. This is more evident in left maxillary teeth 1, 2, 4 and 7.

Dentary teeth mostly resemble the general conditions of the upper jaw teeth. The rostralmost preserved

teeth (at least up to the 7th element) do not show evident crown base constriction. They also have no evidence of denticles, but those are either obscured by concretions, or have worn away. Nonetheless, the denticles are clearly present in teeth from the middle of the dentary tooth series, and in more distal elements.

Axial skeleton: The axial skeleton is preserved in three main articulated groups of vertebrae (Figs 1B, 3E, 4), comprising elements from the trunk series and the sacrum. Two disarticulated mid-caudal vertebrae (one lacking the centrum), scattered haemal arches and fragmented ribs are also referred to the holotype. The sacral and pre-sacral vertebrae were preserved with the ventral surface of the centra facing upwards, and the neural arches and spines of all elements were severely fragmented and worn prior to burial.

The trunk vertebrae were preserved in three semi-articulated segments (Figs 1B, 3E, 4). The caudalmost of those consists of two vertebrae associated to the sacrum. Assuming a priori that *Bagualosaurus agudoensis* originally had 15 trunk vertebrae, as reported to other sauropodomorphs (von Huene, 1926; Galton, 1973; Sereno *et al.*, 2013), these can be identified as trunk vertebrae 14 and 15. More cranially, there is a gap corresponding to at least two vertebrae, and then a segment consisting of three trunk elements. These are tentatively identified as trunk vertebrae 9–11. The cranialmost segment is composed of four vertebrae, displaced from their original position prior to burial. Their anatomy is similar to that of trunk vertebrae 9–10, but their position is more uncertain, and they are referred to as trunk vertebrae A–D.

All preserved trunk centra are spool-shaped (Fig. 3) and amphicoelous, with gently concave articular surfaces. All centra have a pair of lateral depressions, or fossae, one on each side, and these become more evident as the trunk series approaches the sacrum. They show no apertures or any feature that could characterize them as pneumatic (Wedel, 2007). No keels or depressions are seen in the ventral surface of any of the trunk vertebrae. Compared to other sauropodomorphs (Cooper, 1981; Martínez, 2009; Sereno *et al.*, 2013), this suggests that the preserved vertebrae do not belong to the cranialmost part (2–3 first elements) of the trunk series. Regarding their relative proportions, trunk vertebrae located more cranially tend to be lateromedially slenderer. Indeed, 'trunk vertebra A' is the slenderest of all preserved elements with c. 45% the transverse width of trunk vertebra 15 (measured at the midpoint of their centra). The minimum width of the centrum increases in the succeeding vertebrae, with a percentage of c. 70% in 'trunk vertebra B', 'C', 'D', 9, 10 and 11. Trunk vertebra 14 has about the same width of trunk vertebra 15. The centrum is also

proportionally higher in trunk vertebrae 14 and 15, as their height (measured laterally from the ventral tip of the articular surface to the neurocentral junction) reaches about 75% of the craniocaudal length of the centrum. In the other preserved trunk elements, this ratio is c. 45%.

Neurocentral sutures are closed in all preserved trunk vertebrae, but most elements show the contact between the neural arch and the centrum fractured at least in one side. Indeed, the thin lateral walls of the neural canal, as well as the delicate transverse processes and neural spines, were severely affected by biostratinomic agents (e.g. weathering) prior to burial. The preserved trunk vertebrae prezygapophyses extend cranially, surpassing the cranial margin of the centrum and contacting the postzygapophyses of the preceding vertebra by a dorsomedially facing articular surface. The orientation of the prezygapophyses articular facets slightly varies along the trunk series, with the caudalmost elements apparently showing a less oblique articulation relative to the horizontal plane. Yet, the interpretation of such an angle is hampered by the taphonomic distortion suffered by the vertebrae. A lateral, sharp ridge extends along the lateral surface of each prezygapophysis, reaching to the transverse process. This corresponds to the prezygodiapophyseal lamina (PRDL of Wilson, 1999). The postzygapophyses possess ventrolaterally oriented articular surfaces, matching their respective prezygapophyses. Therefore, the postzygapophyses of the last trunk vertebrae also have less oblique articular surfaces. In an analogue way to the PRDL, the postzygapophyses of each trunk vertebrae also possess a lateral lamina connected to the transverse process, i.e. the postzygodiapophyseal lamina (PODL of Wilson, 1999). Between the postzygapophyses, there is a ventrally descending sheet of bone that forms the hyposphene. It is not preserved in all trunk vertebrae, but it is unambiguously visible in the 9th element and is probably also present in subsequent ones. The hyposphene presence cannot be determined in more cranial trunk vertebrae. Though the presence of an hypantrum is inferred by the presence of the hyposphene, it is obscured or was not preserved in any vertebrae.

No trunk vertebra has preserved complete parapophyses, diapophyses or transverse processes. Yet, some of the laminae that buttress the ventral surface of the transverse processes can be observed, although partially crushed or deformed in some elements. These laminae are present in all preserved trunk vertebrae, except for the 15th element. The more robust of those laminae is the caudal centrodiaepophyseal lamina (PCDL of Wilson, 1999), which extends ventrocaudally towards the neurocentral suture. The excavated area bounded dorsally by the PODL and ventrally by the

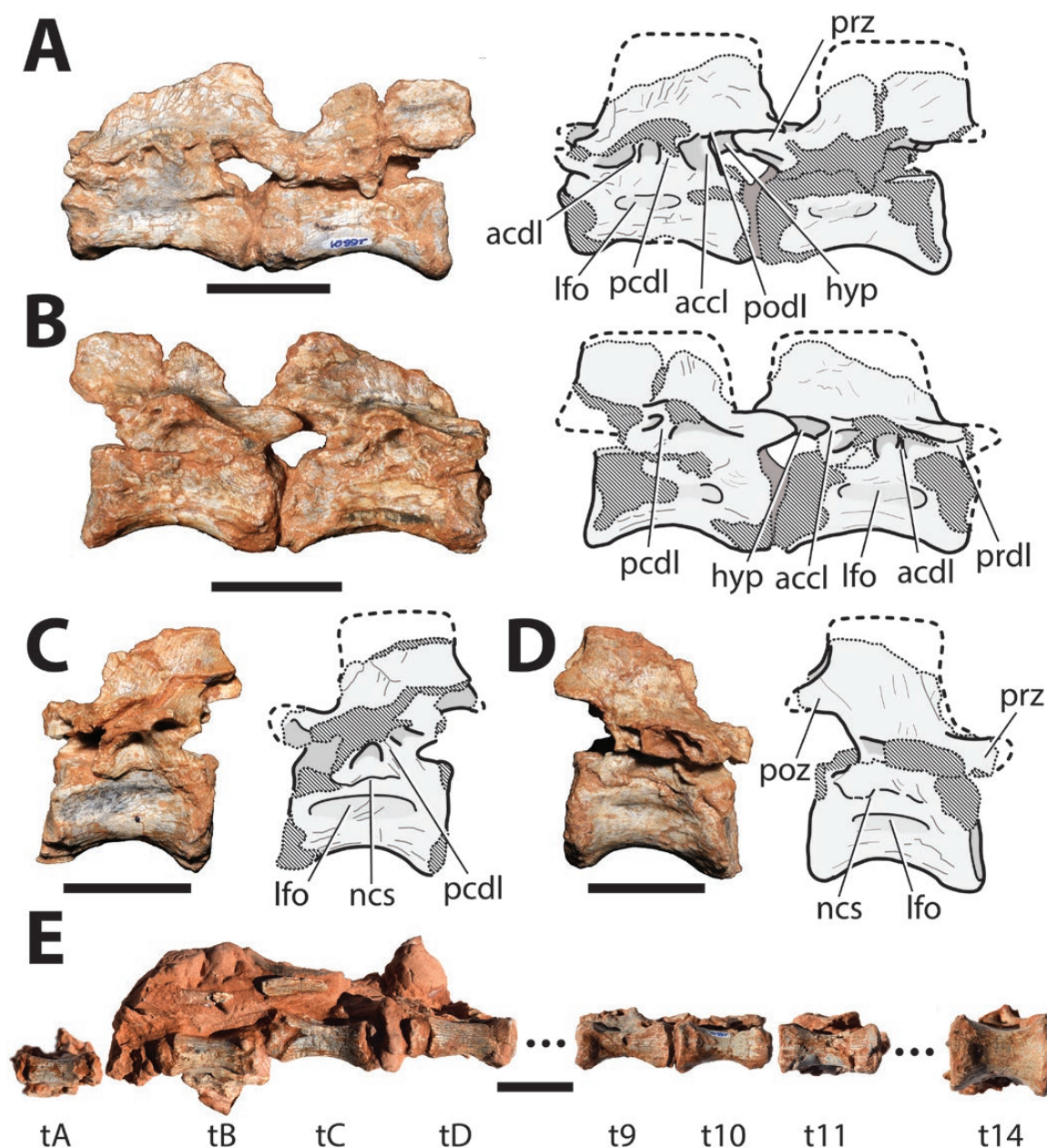


Figure 3. *Bagualosaurus agudoensis* (UFRGS-PV-1099-T), photographs and interpretive drawings of trunk vertebrae 9 and 10 in left (A), and right (B), lateral views; and trunk vertebra 14 in left (C), and right (D), lateral views, respectively. E, sequence of trunk vertebrae, from trunk vertebra A to trunk vertebra 14. Hatched surfaces indicate missing portions, and dashed lines show reconstructions of bone outline. Abbreviations: accl, accessory lamina; acdl, cranial centrodiapophyseal lamina; hyp, hyposphene; lfo, lateral fossa; ncs, neurocentral suture line; pcdl, caudal centrodiapophyseal lamina; poz, postzygapophysis; prdl, prezygodiapophyseal lamina; prz, prezygapophysis; t, truncal vertebra. Scalebars: 2cm.

PCDL forms the caudal chonos. Caudal to the PCDL, and ventral to the PODL, there is an accessory, almost vertical lamina that extends towards the neurocentral suture and effectively divides the caudal chonos in two. Cranial to the PCDL and caudal to the PRDL, there is a very thin lamina that originates from the ventral surface of the transverse process, and extends

cranioventrally towards the neurocentral suture. It is much damaged in all preserved trunk vertebrae of *Bagualosaurus agudoensis*, and referred to here as the cranial (anterior) centrodiapophyseal lamina (ACDL of Wilson, 1999), as observed in trunk vertebrae 9 and 10 (Fig. 3A). The deep ventral chonos is bounded cranially by this lamina and caudally by the PCDL. Although

deep, the ventral chonos does not perforate the neural arch, so that there is no evidence of pneumaticity in the trunk vertebrae of *B. agudoensis*. The cranial chonos is bounded caudally by the ACDL and dorsally by the PRDL. It is relatively shallow compared to the other chonoe.

All preserved trunk vertebrae have incomplete neural spines. They are craniocaudally long, spanning about 80–90% of the respective centrum length, with the more caudal elements having craniocaudally shorter spines, which tend to dislocate caudally in vertebrae closer to the sacrum. On the contrary, the height of the neural spines cannot be established for any of the trunk vertebrae. Caudally, the base of the neural spines is excavated by a medial groove that separates the postzygapophyses from one another, which is more evident in the last trunk vertebrae. Again, given the incompleteness of the preserved neural spines, the dorsal extent of this groove cannot be fully established.

The sacrum of *Bagualosaurus agudoensis* is composed of two primordial sacral vertebrae, plus one additional caudosacral vertebra (Fig. 4). The sacrum and ilia are associated in UFRGS-PV-1099-T, but they are not in their original position (Fig. 1B). As with the trunk vertebrae, the sacral elements are much damaged and their transverse processes, ribs and neural spines are significantly worn. The last trunk vertebra was preserved in articulation with the sacrum, but did not contact the ilium. Indeed, the preserved base of the transverse process of trunk vertebra 15 indicates that it was very slender, like that of the preceding vertebrae. In contrast, the first and second sacral vertebrae bear massive transverse processes and ribs, which formed a broad pelvic articulation. The first caudal vertebra is firmly associated with the second primordial sacral vertebra, and located within the limits of the postacetabular ala of the ilium. Although broken at their bases, its transverse processes seem massive compared to those of the trunk vertebrae, suggesting

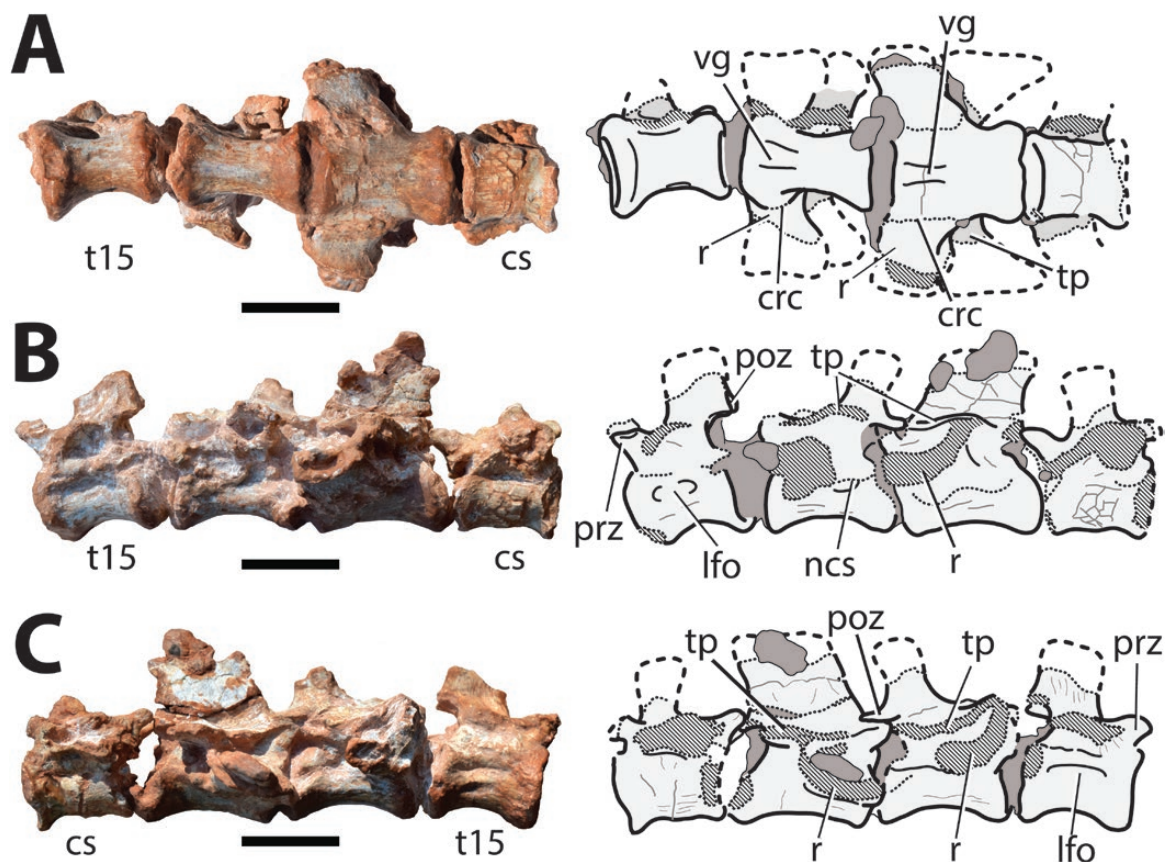


Figure 4. *Bagualosaurus agudoensis* (UFRGS-PV-1099-T), photographs and interpretive drawings of trunk vertebra 15 and sacral vertebrae in ventral (A), left lateral (B), and right lateral (C), views. Hatched surfaces indicate missing portions, and dashed lines show reconstructions of bone outline. Dark grey areas represent the sediment or concretion. Abbreviations: crc, contact between sacral rib and its respective vertebral centrum; cs, caudosacral; lfo, lateral fossa; ncs, neurocentral suture line; poz, postzygapophysis; prz, prezygapophysis; vg, ventral groove; t15, trunk vertebra 15; tp, transverse process; r, rib. Scalebars: 2cm.

that at least the first tail vertebra was recruited into the sacrum, i.e. a caudosacral.

The first primordial sacral centrum is craniocaudally long, slightly surpassing the length of the last two trunk centra. Other than that, it resembles that of trunk vertebra 14 in general proportions. On the contrary, the second sacral vertebra has a transversely widened and dorsoventrally low centrum. It is also craniocaudally long; indeed, it is the longest preserved centrum of UFRGS-PV-1099-T. The caudosacral centrum is, by contrast, the shortest. The ventral surface of both primordial sacral vertebrae bears a very faint longitudinal groove, which is apparently absent in the caudosacral element. The lateral surface of the sacral centra shows no sign of the lateral depressions shared by the trunk vertebrae. The articular surfaces of the two primordial sacral centra are elliptical and dorsoventrally flattened, as is the cranial articular surface of the caudosacral centrum. Yet, its caudal articular surface is subcircular, as those of the trunk vertebrae. There is no evidence of fusion between any of the sacral elements.

The preserved pre- and postzigapophyses of the primordial sacral vertebrae and the caudosacral element have slightly oblique articular surfaces, resembling those of the last two trunk vertebrae. The neural spines are dorsally incomplete, but the preserved bases show that they were narrow, like those of the preceding vertebrae. The first sacral and the caudosacral vertebrae have craniocaudally short neural spines. Comparatively, they are shorter than those of any of the preserved trunk vertebrae, and are restricted to the caudal half of the vertebrae. The second sacral

vertebra, on the contrary, has a craniocaudally long neural spine that spans along most of the vertebral length.

The most distinctive features of the sacral vertebrae are related to the complex structure of their transverse processes and ribs, modified by the articulation to the pelvis. These structures were significantly damaged prior to burial, but some anatomical traits were preserved. The transverse process of the first sacral vertebra is a dorsoventrally thin sheet of bone that projects laterally from the neural arch. Only the caudal part of the left transverse process was preserved, which was lost in the right side. As a whole, the transverse process spans from the lateral surface caudal to the prezigapophysis to roof the intercostals space adjacent to the vertebra, but its entire lateral extent cannot be determined. Yet, the caudal margin of the process arches caudally. Most of the first sacral ribs were worn away, only some parts remaining on the right side. The rib was massively built, spanning from the cranial two-thirds of the lateral surface of the neural arch/centrum to describe an arch as it extends ventrally and caudally. The centrum/rib contact of the first sacral vertebra is clearly seen ventrally, suggesting that both elements were not completely coossified in UFRGS-PV-1099-T. The exact shape of the articular facet that contacted the ilium is unclear, but a splinter of bone, still attached to the medial surface of the preacetabular ala of the ilium, apparently represents a fragment of the first sacral vertebra (Fig. 6B).

The transverse process of the second sacral vertebra is partially preserved in both sides. It also consists

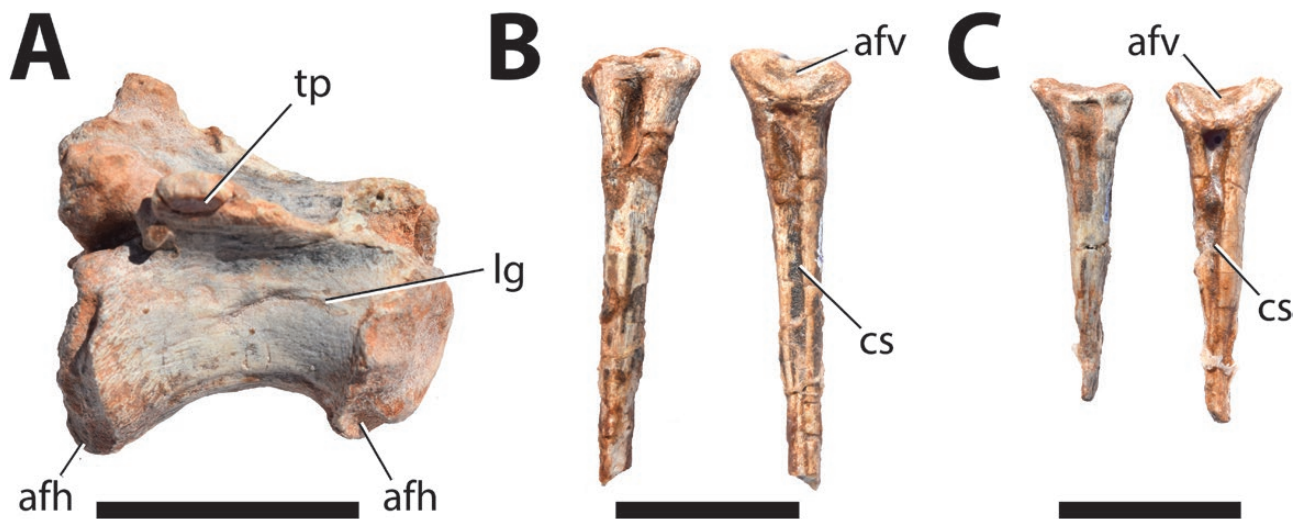


Figure 5. *Bagualosaurus agudoensis* (UFRGS-PV-1099-T), photographs of a caudal vertebra in right lateral view (A), and haemal arches (B, C), in cranial (left) and caudal (right) views. Abbreviations: afh, articular facet for haemal arches on vertebra; afv, articular facet for the vertebral centrum on haemal arch; cs, caudal sulcus; lg, lateral groove on the centrum; tp, transverse process. Scalebars: 2cm.

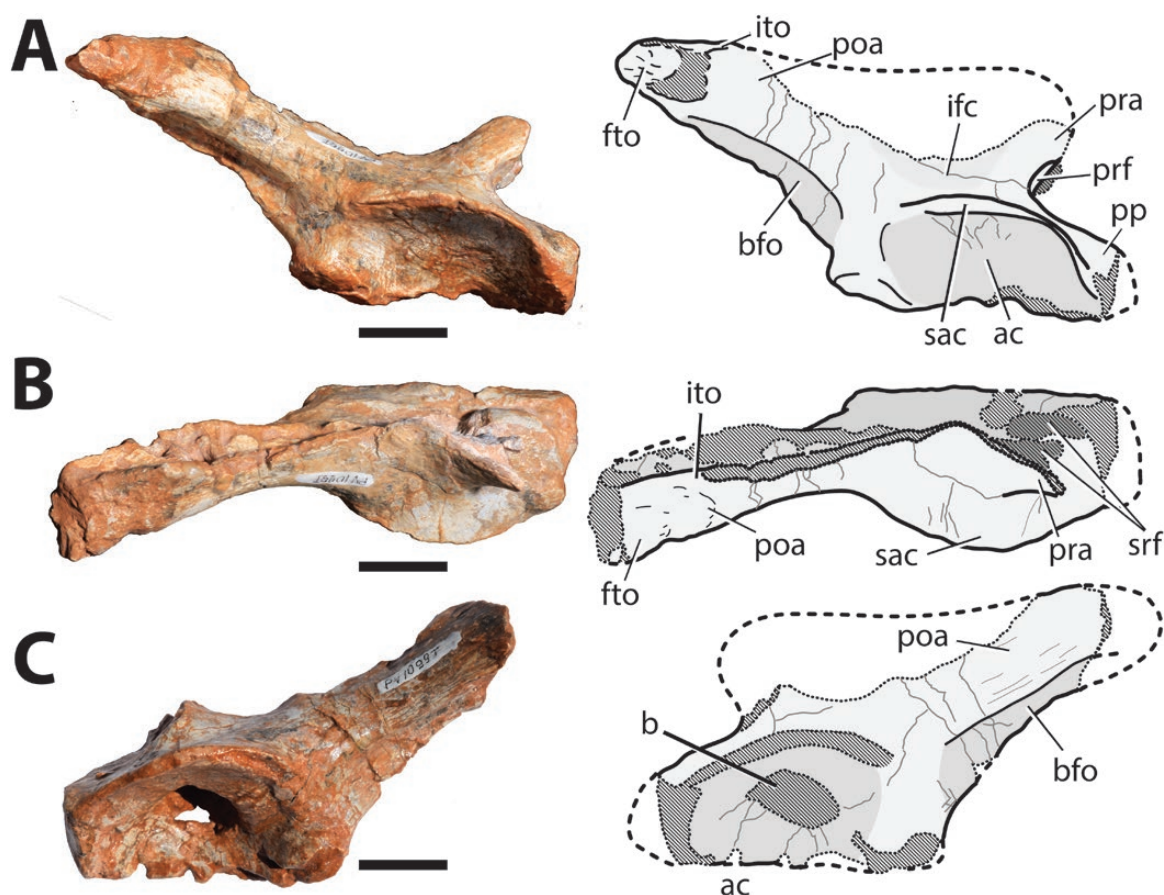


Figure 6. *Bagualosaurus agudoensis* (UFRGS-PV-1099-T), photographs and interpretive drawings of the right ilium in lateral (A), and dorsal (B), views; and left ilium in lateral view (C). Hatched surfaces indicate missing portions, and dashed lines show reconstructions of bone outline. Abbreviations: ac, acetabular surface; b, bore in the acetabulum; bfo, brevis fossa; fto, area of origin of m. femorotibialis; ifc, area of origin of m. iliofemoralis cranialis; ito, area of origin of m. iliotibialis; poa, postacetabular ala; pp, pubic peduncle; pra, preacetabular ala; prf, preacetabular fossa; sac, supracetabular crest; srf, sacral rib fragment. Scalebars: 2 cm.

of a dorsoventrally thin sheet of bone, caudally tapering in dorsal view. Its rib is more massive than that of the preceding vertebra, but its articulation with the centrum is also incompletely fused. As seen in ventral view, the second sacral rib projects laterally and cranially, and its cranial margin probably contacted the first sacral centrum. It is ventrally bowed as seen laterally, extending from the cranial portion of the centrum and reaching the transverse process at the midlength of the vertebra. However, much of the lateral portion of the second sacral ribs, including the articular facets, is significantly damaged. The transverse processes of the caudosacral vertebra are mostly missing, but their preserved bases show that they were robust. Although placed well within the limits of the postacetabular ala, its relation to the ilia is uncertain.

The caudal series of *Bagualosaurus agudoensis* is represented by two vertebrae: one mostly complete

(Fig. 5A) and the other lacking the centrum. Both vertebrae are similar in size, the incomplete element being only slightly shorter. The transverse processes of both vertebrae project and taper laterocaudally and are not ventrally buttressed by laminae. The dorsally tapering neural spines are also caudally sloped. The prezygapophyses are incomplete in both elements, and the postzygapophyses are placed high into the neural spine, with nearly horizontal articular facets. There is no evidence of hyposphene and the preserved centrum is amphicoelic and spool-shaped, with some lateral compression (possibly a post-burial alteration). A shallow groove extends along its lateral surface, similar to those seen in trunk vertebrae. The cranial and caudal surfaces of the centrum are slightly bevelled ventrally, creating the articular surfaces that received the haemal arch. The neurocentral suture is completely closed and, contrasting with the trunk vertebrae, the

boundary between the centrum and the neural arch is not clear in the more complete caudal vertebra.

Two disarticulated haemal arches (Fig. 5B, C) were preserved in UFRGS-PV-1099-T. Their proximal portions are lateromedially expanded, forming the articular surface. Judging from the shape of the articular facets, the preserved haemal arches were probably slightly inclined caudally. The haemal canal is dorsally closed. When observed in cranial/caudal views, the haemal arch tapers towards the distal tip, but its craniocaudal width is relatively constant. They are slightly bowed caudally, as seen in lateral view, and its caudal surface bears a distinct longitudinal groove that extends distally from the distal portion of the haemal canal. Both haemal arches lack their distal tips, so that their total length cannot be assessed.

Trunk ribs are poorly preserved in UFRGS-PV-1099-T, represented only by fragments. These are mostly subcircular in section, some preserving signs of a shallow caudal longitudinal groove. The ribs become progressively more flattened towards their distal end. A single rib shows parts of its two-headed proximal portion. It was preserved close to the cranialmost trunk series, but bears no signs of articulation with the vertebrae. It also bears a longitudinal groove, which extends ventral to the proximal portion, and gradually shifts to a caudoventral position.

Several thin, rod-like elements were preserved in a v-shaped orientation. They are interpreted as part of the gastralia, and referred to the specimen. Yet, it is important to notice that they were not preserved close to their anatomical position, although the distal portions of at least three disarticulated trunk ribs were preserved close to these elements. The gastral rods have less than 25% of the width of the trunk ribs, and are nearly straight for all their preserved length.

Pelvic girdle: The pelvic girdle of *Bagualosaurus agudoensis* is represented by the two ilia and a partial pubis. The right ilium is more complete than the left element, but both lack most of the dorsal lamina. The left ilium bears a large rounded bore in the acetabular wall. It is 18 mm in diameter and its morphology is incompatible with chambers produced by invertebrates. This perforation might be pathological, but further analyses are necessary to fully assess its origin. The pubis was preserved slightly displaced, covering the ventral portion of the right ilium (Fig. 1B). The thin medial lamina that formed the pubic apron was mostly lost during collection.

The ilium (Fig. 6) is craniocaudally elongated, approximately as long as four and a half vertebral centra. The dorsal iliac lamina is medially arched, creating a lateral concavity (Fig. 6B) that houses the area of origin of *m. iliofemoralis cranialis* (Langer, 2003).

The deepest point of this concavity is located caudal to the craniocaudal midpoint of the supracetabular crest. The preacetabular ala is very short resembling, as preserved, the ‘western saddle horn’ shape reported for *Guaibasaurus candelariensis* (Langer, de Bittencourt & Schultz, 2011). The perception of this morphology is reinforced by the taphonomic loss of part of the thin dorsal iliac lamina, which also occurs in specimens of *Guaibasaurus candelariensis* (UFRGS-PV-0725-T) and *Silesaurus opolensis* (see Piechowski *et al.*, 2014). The preacetabular ala is laterally buttressed by a strong and broad iliac preacetabular ridge, which is cranially curved as it extends dorsally. The preacetabular ridge laterally bounds a marked excavation in the cranioventral surface of the preacetabular ala. This may be correspondent to the preacetabular fossa (Hutchinson, 2001a), as recognized in other early dinosaurs (Langer, 2003; Langer *et al.*, 2011). The craniocaudally long postacetabular ala corresponds to 45% of the total iliac length, and is dorsocaudally sloped. In dorsal view, it is also gently bent laterally. Its lateral surface bears a robust brevis shelf that separates the origin area of *m. iliofemoralis cranialis*, dorsally, from the brevis fossa, which is well developed and extends along most of the ventral surface of the postacetabular ala. Medially, the brevis fossa is limited by a vertical bone wall, which spans from the caudal margin of the ischiadic peduncle and tapers towards the caudal end of the postacetabular ala. Its ventral margin corresponds to the ventral margin of the ala in taxa that lack a well-developed brevis shelf. Most of the brevis fossa is exposed in lateral view, except for its caudalmost portion, which is overlapped by a ventrolateral expansion of the brevis shelf. This expansion is contiguous to a rough surface, related to the attachment area of *mm. iliotibialis* and *flexor tibialis* (Langer, 2003; Langer *et al.*, 2011).

The pubic peduncle is elongated, and extends further cranially than the preacetabular ala. It is cranioventrally directed, forming a 25-degree angle to the inferred horizontal plane. The peduncle is mediolaterally wide, and its dorsal surface is gently convex. There is no keeled surface dorsal to the pubic peduncle. The articular facet for the pubis is badly preserved. It faces cranioventrally, but it is impossible to assess its precise slope. A strong supracetabular crest extends caudally from the pubic peduncle, separating the dorsal iliac lamina from the acetabulum. Its lateral expansion is subequal to the dorsoventral depth of the iliac portion of the acetabulum. The cranial portion of the crest is sharp and ventrally sloped, following the cranial margin of the acetabulum. The portion of the crest dorsal to the acetabulum is almost parallel to the horizontal plane, and the preserved lateral rim of the acetabular crest does not fold ventrally over the acetabulum. The iliac part of the acetabulum is about twice longer than

deep, and has a smooth and gently concave medial wall. Its surface texture does not allow distinguishing the main articulation for the femoral head from the remainder of the acetabulum (see Langer, 2003). Its ventral margin, as preserved, is straight above the puboischial junction. The ischiadic peduncle is short and robust, and its cranial portion is dominated by the antitrochanter. The articular facet for the ischium faces ventrally, and is mostly positioned ventral to the antitrochanter. It is partially worn in both ilia, but its ventral outline, as preserved, is sub-rectangular with a rounded lateral margin.

Part of the right pubis (Fig. 7) is preserved in UFRGS-PV-1099-T. The proximal portion is complete, but much of the pubic apron was lost. The pubis/ilium articular surface is incomplete in both bones, hampering the inference of the exact slope of the pubic axis. Although lacking much of the obturator plate, the proximal pubic body preserved the small caudal process that articulates with the ischium, separated from the main pubic body by a distinct ischio-acetabular groove that perforates the lateral wall of the bone. The caudal process exhibits a subtriangular articular facet for the ischium. A sharp crest on the ventromedial

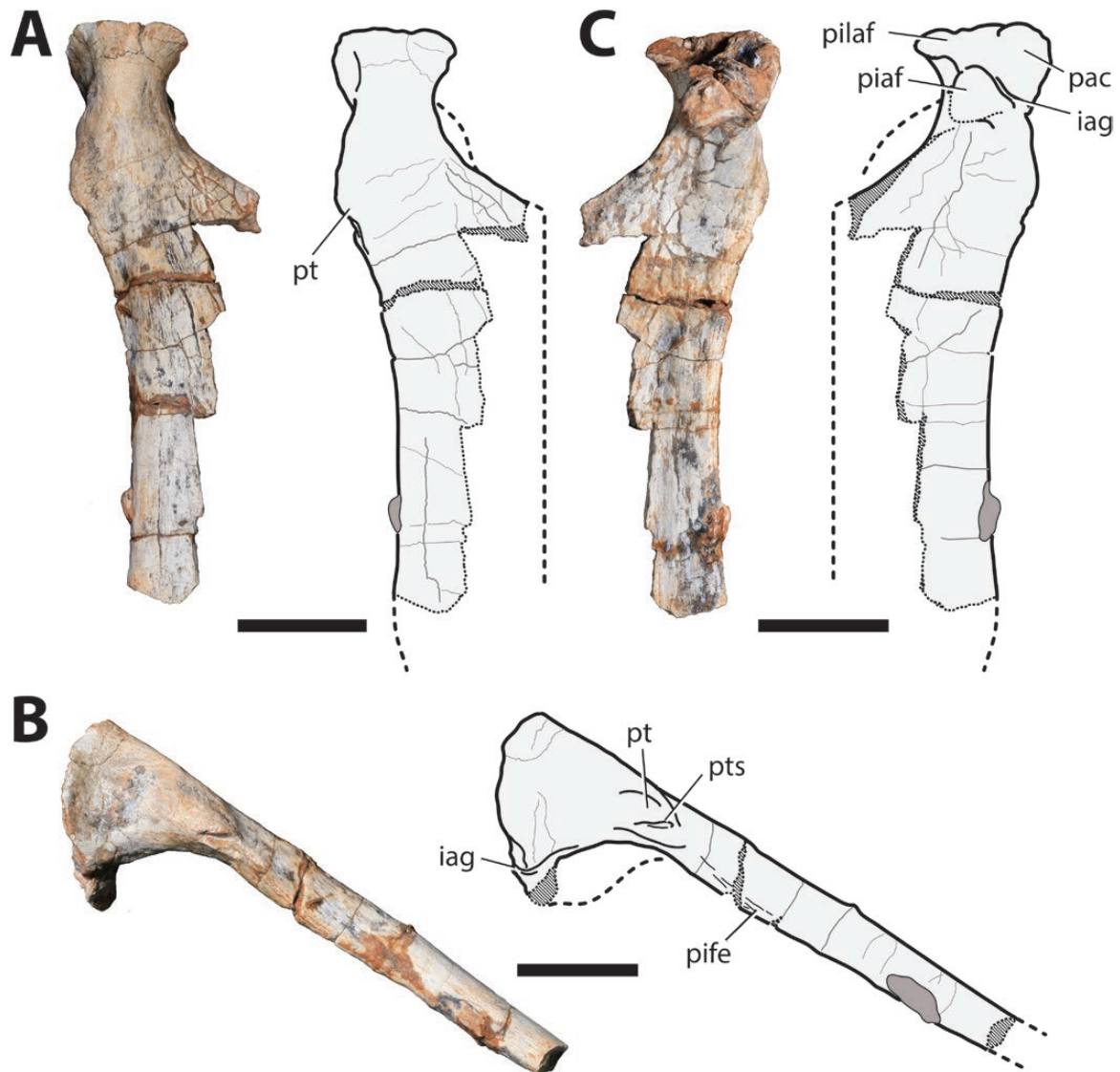


Figure 7. *Bagualosaurus agudoensis* (UFRGS-PV-1099-T), photographs and interpretive drawings of the right pubis in cranial (A), lateral (B), and caudal (C), views. Hatched surfaces indicate missing portions, and dashed lines show reconstructions of bone outline. Dark grey areas represent the sediment or concretion. Abbreviations: iag, ischio-acetabular groove; pac, acetabular surface of the pubis; piaf, articular facet for the ischium on pubis; pilaf, articular facet for the ilium on pubis; pt, pubic tubercle; pts, sulcus on the pubic tubercle. Scalebars: 2 cm.

surface of the pubic caudal process marks the lateral border of the obturator foramen. The dorsocranial surface of the pubic body is very robust, forming a strong buttress, where a set of longitudinal rugosities suggest muscle attachments and a slight concavity excavates the lateral surface of the pubic body. Ventral to this, and somewhat contiguous to the rugosities of the cranial buttress, there is a strongly striated, knob-like bone swelling. This corresponds to the pubic tubercle, or 'ambiens process' (Hutchinson, 2001a; Langer, 2003), which is frequently associated with the origin of *m. ambiens*. The pubic tubercle of *Bagualosaurus agudoensis* is notable for a deep, longitudinal groove along its surface. This is ventrolaterally concave, fitting the inferred orientation of *m. ambiens* (Hutchinson, 2001a; Langer, 2003). Nevertheless, as discussed by Hutchinson (2001a), the correlation of soft tissues to the pubic tubercle is not so simple, and several pubic ligaments, as well as abdominal muscles, could also have attached to that area. There is also the possibility that *m. ambiens* had a double head (as in crocodiles), with a dorsal attachment in the rugosities of the cranial buttress, and a second ventrolateral fixation in the pubic tubercle (see discussion in Langer, 2003). Most of the pubic shaft, particularly the medial pubic lamina, is missing. It is straight in lateral view, and its cross-section is lacrimiform, with the slenderer portion forming the thin medial lamina or 'pubic apron'. A slight rugosity extends ventral from the pubic tubercle, marking part of the lateral margin of the pubic shaft. It may be related with the attachment of part of the part 1 of *m. pubo ischio femoralis externus*, which was inferred for *Saturnalia tupiniquim* (Langer, 2003) to have its most proximal extension bounded by the pubic tubercle and the longitudinal ridge at the lateroventral portion of the pubic body.

Pelvic limb: The hindlimb elements of *Bagualosaurus agudoensis* are slender and elongated. Both femora are nearly complete, but tibia and fibula are more completely preserved only in the left side, which also includes part of the foot. The preservation of these structures is variable. The right femur is less distorted than its counterpart, and serves as the base for most anatomical interpretations. Information on the epipodial elements is based on both sides, as their preservational conditions complement one another. As estimated, based on the complete left fibula, the epipodium is subequal in length to the femur.

The proximal and distal extremities of both femora are partially worn away (Fig. 8). The right bone shows evidence of osteophagic activity (Paes Neto *et al.*, 2016), which may have contributed, at least in part, to the loss at its extremities. As a whole, the femur has a slender and sigmoid profile. The femoral head is

craniomedially oriented, but other than that, all anatomical information about the proximal articulation of the bone was lost. The cranial trochanter is small, blunt and fully attached to the shaft. It is located at the proximal quarter of the femur, on its craniolateral surface. The adjacent trochanteric shelf extends caudovertrally from the cranial trochanter, and both structures, despite being easily identifiable, are not particularly prominent. A small rough bump corresponds to the dorsolateral trochanter. It is located dorsal to the trochanteric shelf, in the caudolateral margin of the proximal part of the femur. The fourth trochanter occupies the caudomedial surface of the femur. It forms a very robust flange that extends proximodistally for about one-fifth of the total femoral length. Its midpoint is located at about one-third of the preserved femoral length from its proximal tip, and corresponds to the more expanded point of the fourth trochanter, measured perpendicularly from the shaft. The outline of the fourth trochanter differs between the right and left femora. In the right bone, the trochanter appears symmetrical, gently sloped both proximally and distally. In the left element, its proximal portion is crushed and deformed, but the distal portion shows a more abrupt, somewhat pendant corner. The morphology of the left fourth trochanter is more consistent with that of early sauropodomorphs, whereas the symmetrical outline of the right element may be the result of overpreparation or taphonomical distortion. The fourth trochanter rim shows extensive scarring, indicating the insertion area of *m. caudofemoralis brevis*, whereas a marked cranial bump marks the insertion of *m. caudofemoralis longus* (Hutchinson, 2001b; Langer, 2003). The intermuscular lines were partially worn away, and only the proximal, more prominent portions of the cranial and caudolateral lines (Langer, 2003) are clearly seen. The cranial intermuscular line starts distal to the cranial trochanter and, from its craniolateral proximal portion, it extends obliquely across the cranial surface of the femur, towards its distal end. Although the distalmost portion of the intermuscular line cannot be confidently assessed, it apparently ends at the craniomedial portion of the distal third of the bone. The caudomedial crest can be traced from the distalmost part of the trochanteric shelf, extending distally along the caudomedial margin of the shaft and forming an edged surface. Like the cranial line, the caudolateral line can be traced only until the distal third of the femur. The distal portion of the femoral shaft is slightly expanded lateromedially and its cranial surface is flat and featureless as preserved. Little can be said about the distal margin of the femur, as this area was severely damaged in both sides. The popliteal fossa is restricted to the distal quarter of the femur, and separates both condyles in the caudal surface of the bone.

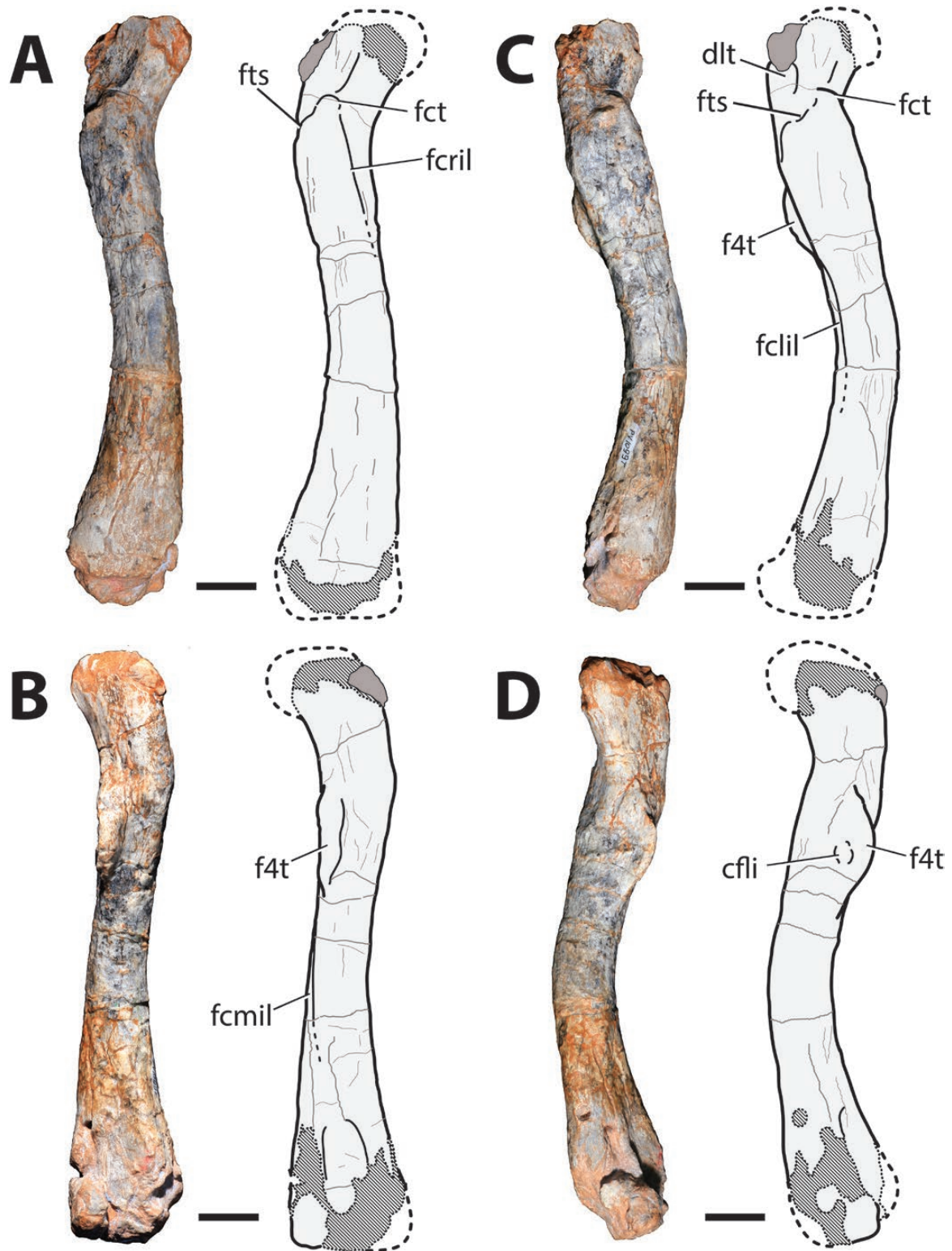


Figure 8. *Bagualosaurus agudoensis* (UFRGS-PV-1099-T), photographs and interpretive drawings of the right femur in cranial (A), caudal (B), lateral (C), and medial (D), views. Hatched surfaces indicate missing portions, and dashed lines show reconstructions of bone outline. Dark grey areas represent the sediment or concretion. Abbreviations: cflil, raised surface for the insertion of *m. caudofemoralis longus*; dlt, dorsolateral trochanter; f4t, fourth trochanter of the femur; fclil, caudolateral intermuscular line; fcmil, caudomedial intermuscular line; fcril, cranial intermuscular line; fct, cranial trochanter of the femur; fts, trochanteric shelf. Scalebars: 2 cm.

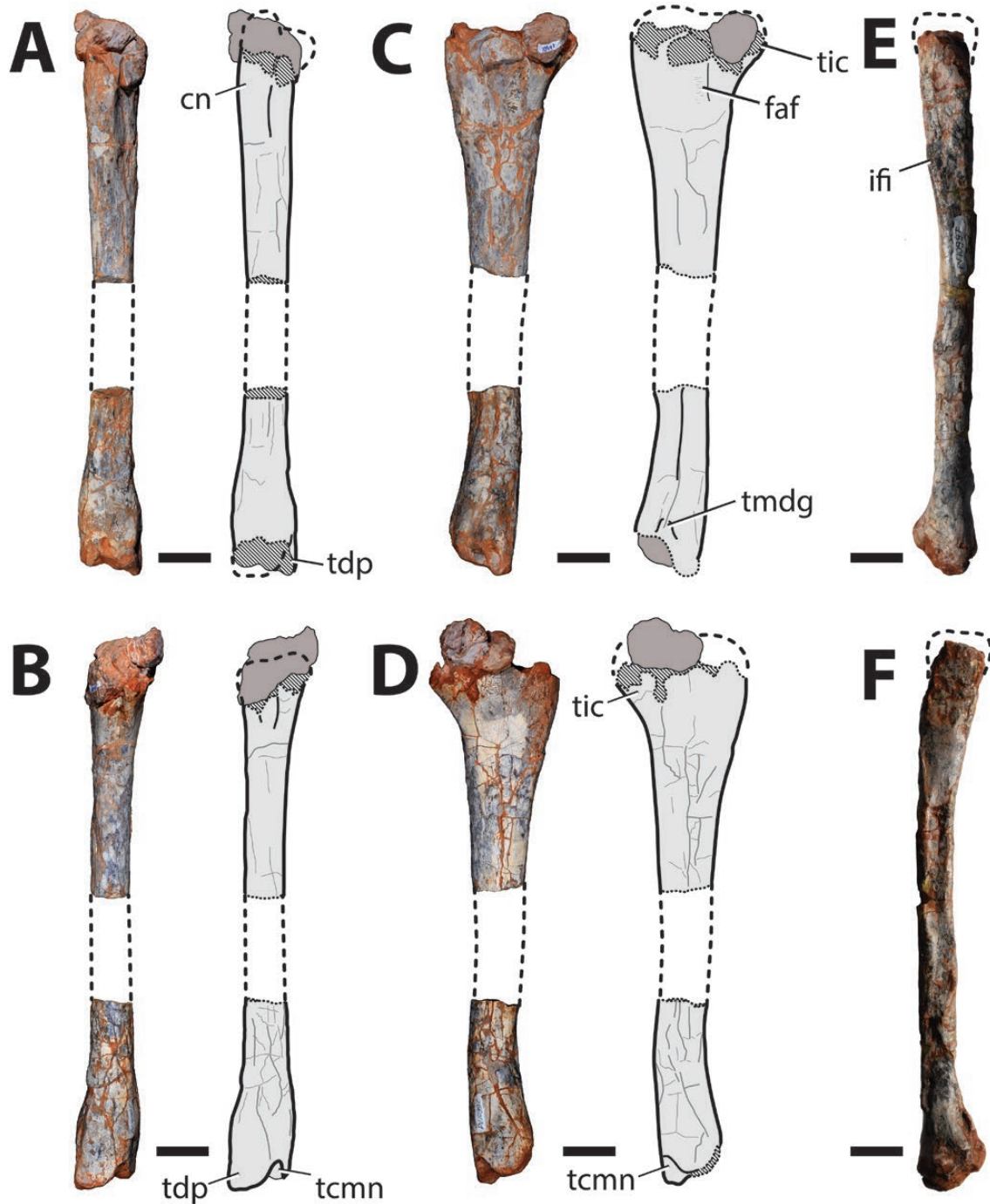


Figure 9. *Bagualosaurus agudoensis* (UFRGS-PV-1099-T), photographs and interpretive drawings of the left tibia in cranial (A), caudal (B), lateral (C), and medial (D), views; and left fibula in lateral (E), and medial (F), views. Hatched surfaces indicate missing portions, and dashed lines show reconstructions of bone outline. Dark grey areas represent the sediment or concretion. Abbreviations: cn, cnemial crest of tibia; faf, articular facet for the fibula; ifi, insertion area for the m. iliofibularis; tcmn, caudomedial notch of distal tibia; tdp, descending process of distal tibia; tic, internal condyle of tibia; tmdg, longitudinal groove at distal tibia. Scalebars: 2 cm.

Both tibiae (Fig. 9A–D) are preserved, but incomplete. The left bone is represented by both proximal and distal extremities, lacking a shaft segment

estimated to be at least 5 cm (the total length of the bone can be inferred from the complete left fibula). The right tibia lacks the distal portion and is somewhat

damaged, especially at its lateral surface. Both tibiae lack the proximal articular surface, but the preserved proximal portion is lateromedially compressed in proximal view, with a medial margin that is convex in the right element and straight in the left. The cnemial crest is cranio-laterally projected and caudally bound, at the lateral surface, by a gentle longitudinal depression. This separates the cnemial crest from the fibular articular facet, which is not strongly marked in the bone surface. The fibular and the internal condyles are separated by a shallow caudal groove. Although poorly preserved, the fibular condyle seems to be larger than the internal condyle. The midshaft cross-section is oval, with a more angled cranial margin and more rounded caudal surface. The bone wall is thick, with the medullary cavity occupying about 50% of the diameter of the shaft. Towards the distal end, the cross-section of the shaft becomes subcircular, and the tibia is slightly lateromedially expanded at its distal portion. The distal outline of the tibia is subquadrangular and the cranial portion of the distal articulation is much damaged, hampering understanding of its relation to the astragalus. Its caudal portion is better preserved, with the descending process projecting distally to articulate to the caudal part of the astragalus proximal surface. The lateral projection of the descending process is very reduced and surely did not overlap the fibula caudally. The lateral surface of the distal part of the tibia bears a longitudinal groove. The caudomedial corner of the tibia appears to be rounded, and there is no evident crested corner. On the contrary, it is excavated by a conspicuous caudomedial notch.

The fibula (Fig. 9E, F) is a long and thin bone, partially preserved in both sides. The left element preserves most of its length, but is somewhat deformed, especially at the proximal portion. The right bone lacks its distal quarter, but shows a better-preserved surface. Like other long bones, both fibulae have severely worn proximal and distal extremities. As preserved, the proximal part of the fibula is cranio-caudally expanded, medially flat, with a convex lateral surface. The medial surface shows some scarring extending distally along the proximal quarter of the bone, starting at its medio-caudal surface and reaching the cranial margin. When in articulation to the tibia, this area is contiguous to the fibular articular facet on that bone, although the distalmost portions of these areas did not contact one another. Such rugosities may indicate the presence of ligaments that helped strengthening the tibio-fibular articulation. The cranial margin of the fibula bears a faint ridge, starting at one-fourth the length from its proximal extremity. It extends distally and becomes progressively fainter, reaching the midpoint of the fibula. This crest corresponds to the insertion of

m. iliofibularis (Langer, 2003), and also marks the portion where the fibula suffers a lateral kink. The fibular shaft is straight for most of its length. The area where the distal part of the fibula contacted the tibia has no distinctive scarring apart from two very faint ridges at the cranial and caudal margins.

No tarsal elements were preserved, but much of the left pes was recovered (Fig. 10). It includes all metatarsals, but with worn away proximal portions. Some phalanges of digits I–IV were also preserved, in articulation to the respective metatarsus. The five metatarsals that compose the pes of *Bagualosaurus agudoensis* are relatively gracile and were preserved in tight association. Metatarsals I and V are the shortest on the series, with metatarsals II–IV being significantly longer; the third metatarsal is the longest of them.

As preserved, the proximal portion of metatarsal I is lateromedially compressed, with a slight cranio-caudal expansion. This creates a broad medial contact with metatarsal II. Metatarsal I is subcircular in cross-section at midshaft, and the distal end is also slightly expanded. It is slightly rotated relative to the rest of the bone, so that the medial condyle is positioned more caudally than the lateral. The distal end of the cranio-medial surface shows a cleft that separates the distal articulation in cranio-lateral and caudomedial surfaces. Proximal to this cleft, a slightly scarred surface marks the extensor depression, which is not excavated as in the other metatarsals. The collateral pit is well developed in the medio-caudal surface of the medial condyle, but the presence of its counterpart in the lateral condyle cannot be assessed, as this area is covered by metatarsal II.

Assuming that the three central metatarsals were not disarticulated prior to burial, and that their proximal ends are proximally aligned, metatarsal II is, as preserved, the shortest of the triplet. Its proximal end is conspicuously expanded cranio-caudally, whereas its mediolateral width is virtually the same along the entire bone. As such, the bone has a subrectangular proximal outline. Its distal end is slightly rotated, but not as strongly as that of metatarsal I, so that the extensor depression faces cranio-medially and the medial condyle projects further caudally. The extensor depression of metatarsal II is markedly excavated and strongly striated, with its margins slightly raised. The distal end of the bone has a minor cranio-caudal expansion, and almost neglectable mediolateral expansion. The medial surface of the medial condyle shows a subcircular pattern of striations, but its collateral pit is not as excavated as in metatarsals I, III and IV. The lateral surface of the lateral condyle cannot be assessed, as it is covered by metatarsal III.

Metatarsal III is the longest of the series. Its proximal portion is lateromedially narrower than that of

metatarsal II, but has a similar craniocaudal expansion. The cranial surface of the shaft is flat, so that the transverse section is subquadrangular. As in metatarsal II, the distal end is only slightly expanded. Its cranial surface is marked by a very deep extensor depression, which forms a deep, extensively scarred

lateromedially expanded groove. Proximal to that, there is a second, less marked excavation. It corresponds to a densely scarred subcircular pit, the bone surface of which is very similar to that of the extensor depression. This suggests that the pit corresponds to an anatomical, rather than taphonomical feature.

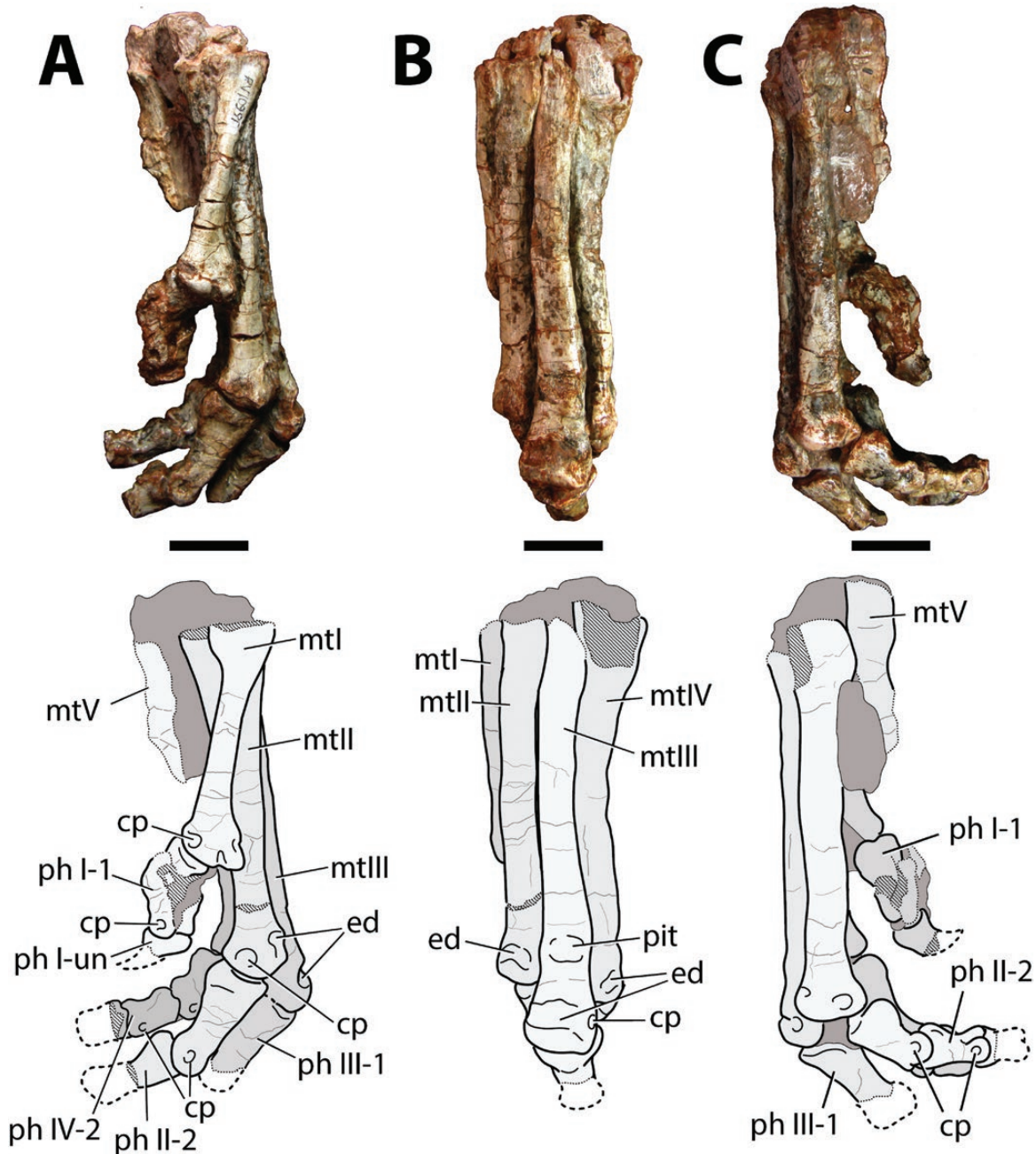


Figure 10. *Bagualosaurus agudoensis* (UFRGS-PV-1099-T), photographs and interpretive drawings of the left pes in medial (A), cranial (B), and lateral (C), views. Hatched surfaces indicate missing portions, and dashed lines show reconstructions of bone outline. Dark grey areas represent the sediment or concretion. Abbreviations: cp, collateral pit; ed, extensor depression; mt, metatarsal; ph, phalanx; pit, additional pit in metatarsal III; un, ungual. I–V, metatarsals or digits I–V. Phalanges indicated by numbers. Scalebars: 2cm.

To our knowledge, such a pit is unique among early dinosaurs, but further data are required to define if it represents an autapomorphy of *Bagualosaurus agudoensis*, or just an aberrant condition of this particular element. The condyles of metatarsal III appear to be symmetrical, but most of their caudal surfaces are obscured by a hard concretion, as well as by metatarsals II and IV. The medial condyle bears a very shallow collateral pit, mainly recognized by its rough, scarred surface. The lateral condyle shows a more conspicuously excavated pit, comparable to that of the medial condyle of metatarsal I, but more densely scarred.

As preserved, metatarsal IV is only slightly more distally projecting than metatarsal II. It is gently bowed medially, creating a concave lateral profile for the shaft. Its proximal surface is the most damaged of all metatarsals, but it is conspicuously expanded lateromedially. The caudolateral corner of the bone bears a concave, proximal surface, which lodged the reduced metatarsal V. Of the three central metatarsals, metatarsal IV shows the least lateromedially expanded distal end. It retains the same midshaft width, with only a slight craniocaudal swelling. The extensor depression is shallower than that of metatarsal II, but the collateral pit of lateral condyle is the deepest of all metatarsals. The medial condyle is hidden by the phalanges and metatarsal III, but it seems only slightly less developed than the lateral condyle.

Metatarsal V is the smallest of all metatarsals, with less than half the length of metatarsal IV. It is severely damaged, with the loss of some portions. Although worn, the proximal surface shows a conspicuous mediocaudal process, that produces an L-shaped proximal outline. This flange tapers distally, not reaching the midshaft of the bone. The craniomedial surface of metatarsal V is flat, matching the caudolateral concavity of the proximal end of metatarsal IV. As preserved, the metatarsal V shaft is lateromedially flattened and tapers distally. There is no evidence of a distal articular surface, indicating that the fifth digit of *Bagualosaurus agudoensis* had no phalanges.

Proximal phalanges of pedal digits I–IV are preserved, but none preserved the full phalangeal formula. The first phalanx of digit I is severely crushed. Based on the shape of the distal articular facet of metatarsal I, the digit movements were probably oblique to the craniocaudal axis, rather describing a craniomedial to caudolateral movement. The medial collateral pit can be readily identified, forming a circular depression. Only the proximal portion of the ungual phalanx of digit I was preserved. It is strongly lateromedially compressed, and possesses a well-developed dorsoproximal prong related to the extensor musculature of the digit. This is the only ungual preserved for *Bagualosaurus agudoensis*.

The first phalanx of digit II is elongated, reaching 37% of the length of its respective metatarsal. Its proximal articular surface is subtriangular and the dorsoproximal corner slightly scarred. The mid-section of the bone is elliptical, and the distal end slightly expanded, with rounded and well-marked collateral pits. A deep extensor depression occupies the dorsal surface of the distal end of the bone. The second phalanx of digit II is incomplete. It also has a triangular proximal articular surface, and the cross-section is subcircular. The cross-section shows no hollow spaces within the bone, which seems very compact at mesoscopic observation. The first phalanx of digit III is also incomplete. It resembles the first phalanx of digit II in all aspects, but is much more robust. Digit IV preserved the first two phalanges, plus a fragment of the third. These phalanges are significantly shorter than the proximal phalanges of other digits. They also show a marked extensor depression at the dorsal portion of the distal end, with well-marked collateral pits. The dorsal surface of the proximal end also shows some scarring, developed as a short prong in the second and third phalanges, probably related to the attachment of extensor musculature.

PHYLOGENETIC ANALYSES

In order to assess the phylogenetic relationships of *Bagualosaurus agudoensis*, the information preserved in the holotype was scored in a modified version of the dataset of [Cabreira *et al.* \(2016\)](#). Apart from the scoring of the new taxon, seven characters not present in the original analysis were added (see [Supporting Information](#)). The analysis was conducted in TNT v.1.5 ([Goloboff, Farris & Nixon, 2008b](#); [Goloboff & Catalano, 2016](#)), following the same protocols employed by [Cabreira *et al.* \(2016\)](#), i.e. ‘Traditional search’ (RAS + TBR); random seed = 0; 5000 replicates; hold = 10. The search resulted in 18 most parsimonious trees of 877 steps (CI = 0.347; RI = 0.637). The strict consensus ([Fig. 11A](#)) shows *B. agudoensis* well-nested within Sauropodomorpha, occupying a position between the Carnian and Norian sauropodomorphs scored in the data matrix. In order to compare results with the other analyses, additional searches were performed adopting extended implied weighting (see below), with default settings and varying values for the constant k ($k = 3$, $k = 7$, $k = 12$). The resulting consensus ([Fig. 11B](#)) does not change the topology significantly from the previous search (with equal weighting), other than resolving some nodes in the silesaurid and ornithischian parts of the tree.

An additional analysis was performed using the dataset of [Ezcurra \(2010\)](#). This dataset, which

represents a compilation of the matrices of [Smith & Pol \(2007\)](#) and [Yates \(2007\)](#), was later modified by other authors ([Novas et al., 2011](#); [Ezcurra & Apaldetti, 2012](#); [Martínez, Apaldetti & Abelin, 2012](#)). The version utilized in this work comprises all these changes, plus some further modifications. These include the rescoring of some taxa, the addition of three new characters and the complete scoring of the holotype of *Bagualosaurus agudoensis* and the early sauropodomorph *Buriolestes schultzi* (see [Supporting Information](#)). The search was also conducted in TNT v.1.5 under the 'Traditional search' algorithm (RAS + TBR) with random seed = 0; 1000 replicates; hold=10, and 37 characters treated as ordered (see [Supporting Information](#)). The search resulted in 280 most parsimonious trees of 1301 steps (CI = 0.348; RI = 0.688), with the strict consensus ([Fig. 12A](#)) recovering *B. agudoensis* nested within a collapsed Eusaurischia. A second analysis (excluding *Agnosphytis cromhallensis* and ISI R277) resolved that polytomy ([Fig. 12B](#)), recovering *B. agudoensis* as the

sister-taxon to post-Carnian sauropodomorphs, agreeing with the analysis based on the dataset of [Cabreira et al. \(2016\)](#). As with the previous analysis, additional searches were conducted adopting extended implied weighting ([Fig. 12C](#); [Supporting Information](#)), adopting varying values for k ($k = 3, k = 7, k = 12$). Though this procedure does not change the nesting of *B. agudoensis* within Sauropodomorpha (i.e. as a sister-taxon to *Pantyraco caducus* and most post-Carnian sauropodomorphs), some variations were observed in the topology, namely the collapse of Dinosauria under $k = 7$ (which does not occur under $k = 3$ and $k = 12$; see [Supporting Information](#)); and the recovery of some early sauropodomorphs (*Buriolestes schultzi*, *Eoraptor lunensis*, *Pampadromaeus barberenai* and *Panphagia protos*) as a distinct clade, sister-group to other sauropodomorphs. This arrangement is also recovered in the analyses adopting $k = 3$ and $k = 12$ (see [Supporting Information](#)).

Following the recent debate on dinosaur origins ([Baron, Norman & Barrett, 2017a, b](#); [Langer et al.,](#)

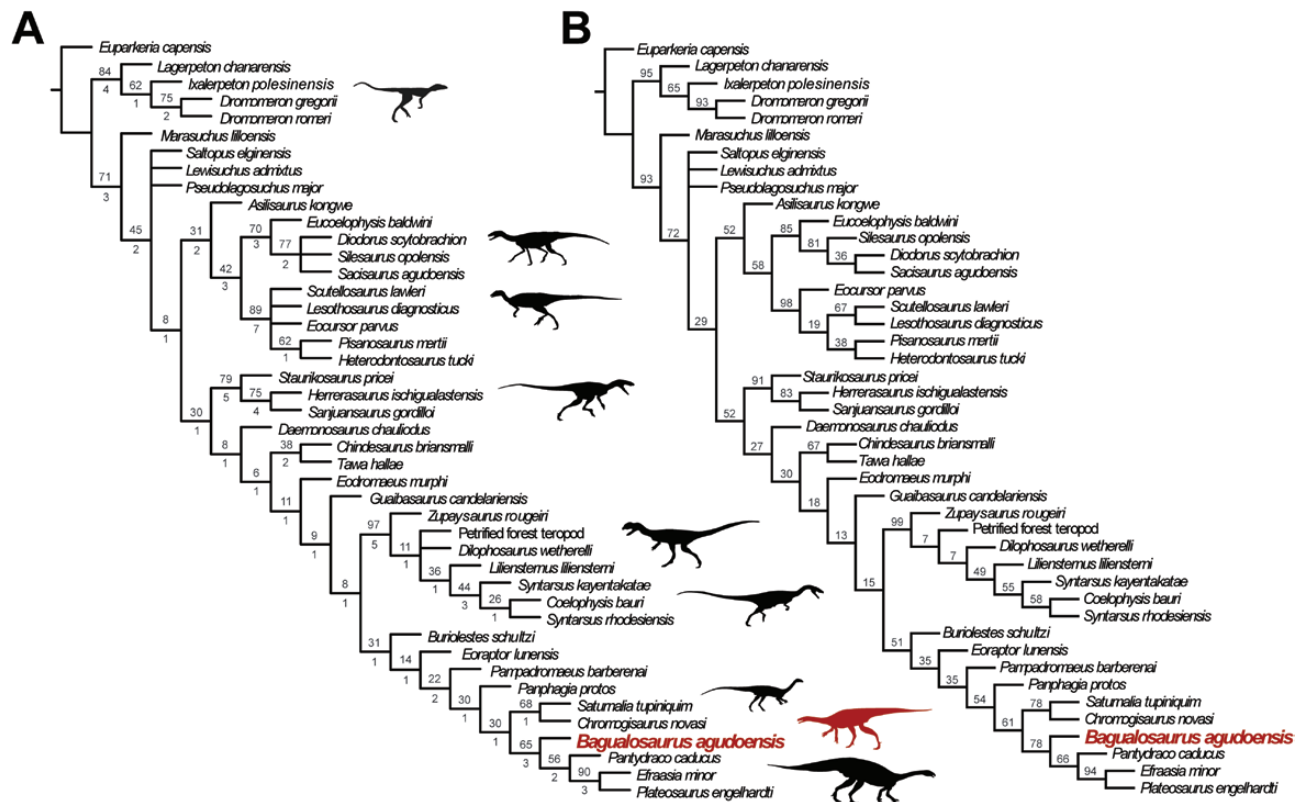


Figure 11. A, strict consensus of the 18 most parsimonious trees recovered in the phylogenetic analysis based on a modified version of the data matrix of [Cabreira et al. \(2016\)](#), with equal weighting. Results show *Bagualosaurus agudoensis* nested within Sauropodomorpha, in an intermediary position between Carnian and Norian sauropodomorphs. Bootstrap values (up) and Bremer Support (under) are indicated at the nodes. Best score = 878 steps; CI = 0.347; RI = 0.637. B, strict consensus of the three most parsimonious trees recovered in the same analysis, but adopting extended implied weighting. Symmetric resampling values shown at the nodes (for the analysis adopting $k = 7$). The recovered topology is the same for the three adopted values of k ($k = 3, k = 5, k = 12$).

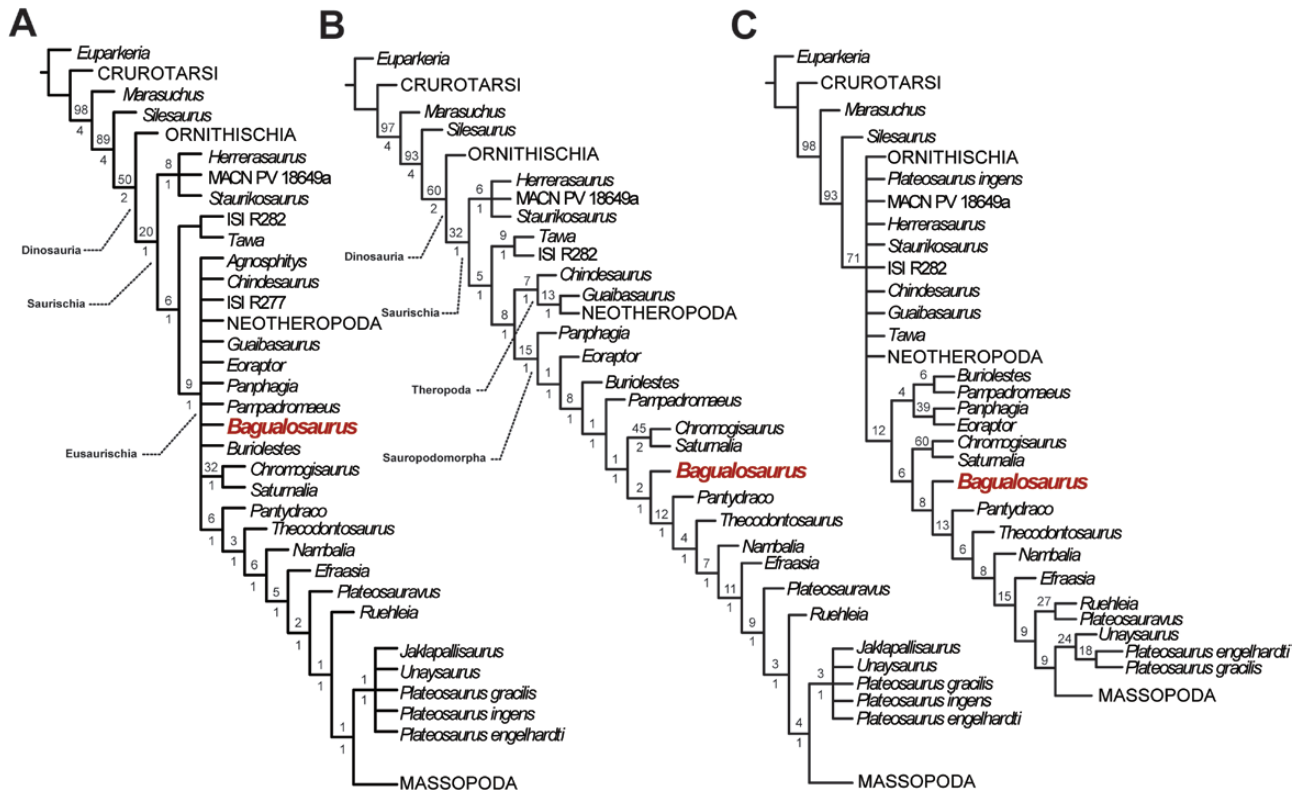


Figure 12. A, strict consensus of the 280 most parsimonious trees recovered in the phylogenetic analysis based on a modified version of the data matrix of [Ezcurra \(2010\)](#). Bootstrap values (up) and Bremer Support (under) are indicated at the nodes. Best score = 878 steps; CI = 0.347; RI = 0.637. B, strict consensus of the same analysis, after the a priori exclusion of *Agnosphytis* and ISI R277 from the analysis. Search resulted in 40 most parsimonious trees of 1300 steps; CI = 0.348; RI = 0.688. C, strict consensus of the 370 most parsimonious trees obtained by the adoption of the extended weighting method ($k = 7$) in the same search, also excluding *Agnosphytis* and ISI R277 from the analysis. Symmetric resampling values shown at the nodes. To reduce image size, all sauropodomorphs recovered within Massopoda were represented as a single terminal. Topologies obtained under other values of k ($k = 3$ and $k = 12$) are provided in the [Supporting Information](#).

2017), a third analysis was conducted, scoring *Bagualosaurus agudoensis* in the dataset of [Baron et al. \(2017a\)](#), as further modified by [Langer et al. \(2017\)](#). The initial search was conducted in TNT v.1.5 under the same parameters adopted by the latter authors (i.e. a 'New Technology Search' combining Wagner trees, TBR branch swapping, sectorial searches, Drift and Tree Fusing, conducted until the achievement of 100 hits of the same minimum length; this was followed by a final round of TBR branch swapping based on the trees obtained on the first analysis). The search resulted in 110 316 most parsimonious trees of 1939 steps (CI = 0.276; RI = 0.606), the consensus of which recovers the classical Ornithischia–Saurischia dichotomy. Early saurischians, however, were recovered nested in an extensive polytomy (Fig. 13A). As discussed elsewhere ([Baron et al. 2017b](#); [Langer et al., 2017](#)), dataset construction, missing data and homoplasy may be major causes for ambiguous and poorly supported

topologies. Therefore, in an attempt to improve the results, as well as testing the effect of these factors in the analysis, additional searches were conducted employing implied character weighting against homoplasy. Previous authors (e.g. [Goloboff et al., 2008a](#); [Legg, Sutton & Edgecombe, 2013](#); [Goloboff, 2014](#)) suggest that weighting should be applied in datasets with potential homoplasy, such as morphological or palaeontological datasets. In addition, the extended implied weighting method ([Goloboff, 2014](#)) deals with the potential artificially inflated weights that could arise from missing data in the datasets, a common case in palaeontological data matrices. The additional searches were conducted employing three different values for the concavity constant k ($k = 3$, $k = 7$ and $k = 12$). As in the analyses adopting alternative datasets, this search recovered *Bagualosaurus agudoensis* as the sister-taxon to post-Carnian sauropodomorphs for all adopted values of k (Fig. 13B; [Supporting Information](#)). One unexpected result, however, was

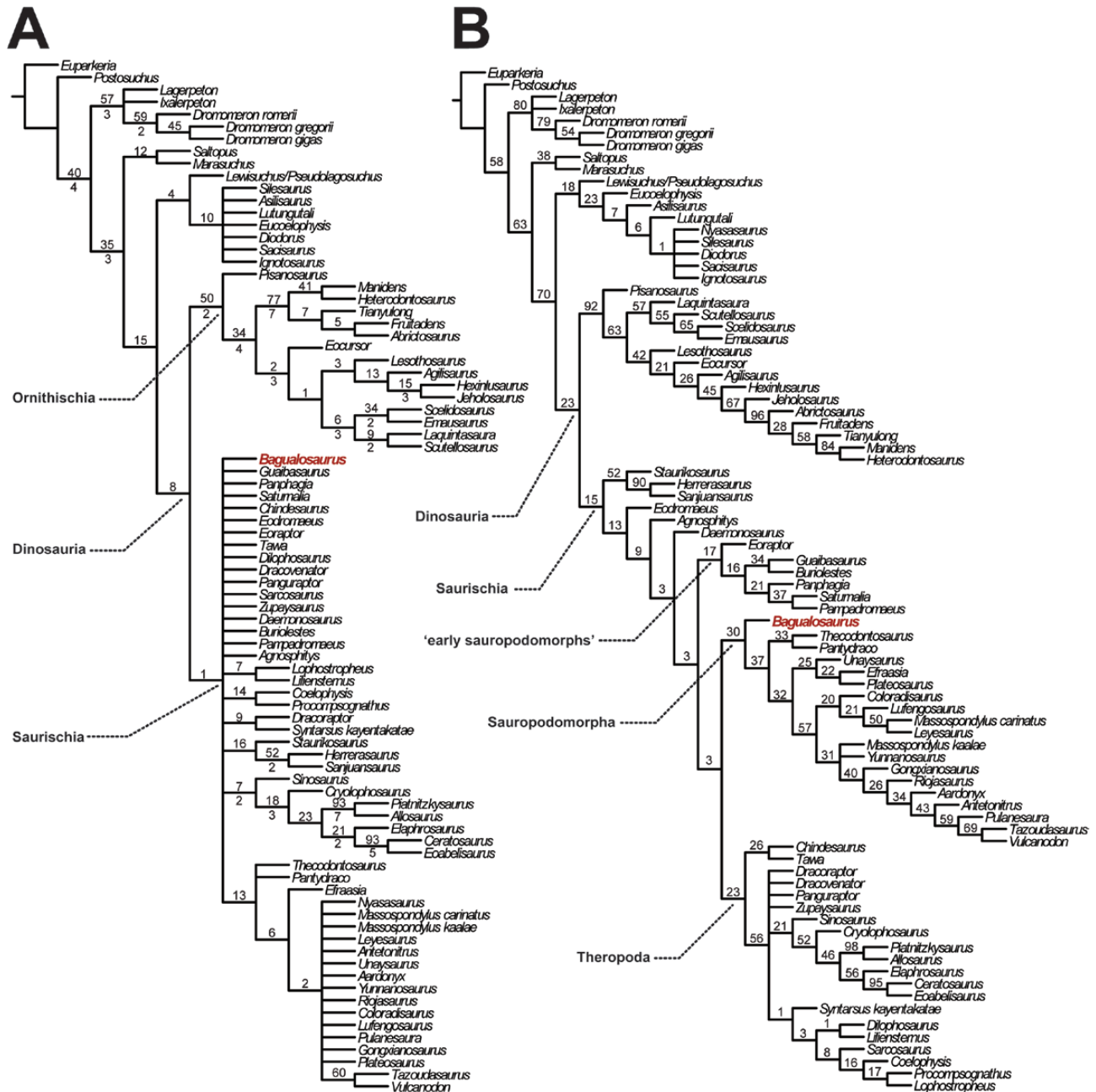


Figure 13. A, strict consensus of the 110316 most parsimonious trees recovered in the phylogenetic analysis based on the dataset of Baron *et al.* (2017), as modified by Langer *et al.* (2017). Bootstrap values (up) and Bremer Support (under) are indicated at the nodes. Best score = 1939 steps; CI = 0.276; RI = 0.606. B, strict consensus of the 35 most parsimonious trees obtained by the adoption of the extended weighting method ($k = 7$). Topologies obtained under other values of k ($k = 3$ and $k = 12$) are provided in the [Supporting Information](#).

the recovery of some taxa traditionally recognized as ‘early sauropodomorphs’ as a clade that falls basal to the Theropoda–Sauropodomorpha dichotomy. Under $k = 7$ (Fig. 13B) and $k = 3$ (see [Supporting Information](#)), this clade also includes *Guaibasaurus candelariensis*, thus forming the family Guaibasauridae (Ezcurra,

2010). Nonetheless, under the higher value $k = 12$ ([Supporting Information](#)), these ‘early sauropodomorphs’ are again nested within Sauropodomorpha, while *G. candelariensis* groups with theropods. Goloboff, Torres & Arias (In press) point out that, for larger datasets, higher values of k tend to perform

better than strong concavities (like $k = 3$ or $k = 7$). Despite that, the different topologies recovered under different values of k reinforce the idea that analyses of early dinosaur evolution may be significantly affected by incompleteness of specimens (i.e. missing data), as well as homoplasy, agreeing with Langer *et al.* (2017) and Baron *et al.* (2017b).

DISCUSSION

Bagualosaurus agudoensis has a unique combination of characters that allows its differentiation from all known coeval sauropodomorphs, as well as from other representatives of the group. Apart from having several synapomorphies that are widely shared among Sauropodomorpha, the new taxon has a combination of plesiomorphic traits that are retained only in early members of the group (i.e. Carnian taxa) with traits that were thought to appear only in later (post-Carnian) sauropodomorphs.

One of the main differences of *Bagualosaurus agudoensis* relative to coeval sauropodomorphs is the significantly larger body size of the new taxon. With a femoral length of at least 215 mm, *B. agudoensis* is at least 25–50% larger than any other Carnian sauropodomorph (Langer, 2003; Ezcurra, 2010; Cabreira *et al.*, 2011, 2016; Sereno *et al.*, 2013). It shares with *Saturnalia tupiniquim* a subequally long femur and epipodium, a feature retained among Norian sauropodomorphs, but also present in *Guaibasaurus candelariensis* and larger dinosaurs. This contrasts with other early sauropodomorphs (and most small-sized dinosauromorphs) that reportedly have elongated epipodials. The relative reduction in epipodial length appears to be related to an increased body size, both in post-Carnian sauropodomorphs and large theropods (Nesbitt, 2011). Yet, as recognized by Nesbitt (2011), this is certainly not the case in *S. tupiniquim*. Therefore, it is reasonable to assume that, at least in sauropodomorphs, the relative shortening of the epipodium evolved prior to the acquisition of a large body mass. Indeed, the hindlimbs of both *S. tupiniquim* and *B. agudoensis* are composed of gracile bones, resembling more those of early sauropodomorphs than more advanced members of the group.

Among Sauropodomorpha, the skull of *Bagualosaurus agudoensis* has a combination of plesiomorphic and derived features that is consistent with its intermediary phylogenetic position between coeval Carnian sauropodomorphs and Norian forms (Fig. 11). The first premaxillary tooth of *Bagualosaurus agudoensis* has a relatively high crown, as better observed in the left side of the skull of the holotype (Fig. 2), and no teeth along the maxillary series surpass the crown height of that tooth. Among the sauropodomorphs sampled for the phylogenetic analysis, this trait is

reported only for *Pantyraco caducus*, *Efraasia minor* and *Plateosaurus engelhardti* (Galton, 1985; Yates, 2003a, b; Galton & Kermack, 2010), but also occurs in *Massospondylus carinatus* (Sues *et al.*, 2004) and possibly *Adeopapposaurus mognai* (Martínez, 2009). In the coeval sauropodomorphs *Pampadromaeus barberenai*, *Eoraptor lunensis* and *Buriolestes schultzi* (Cabreira *et al.*, 2011, 2016; Sereno *et al.*, 2013), the first premaxillary tooth has a short crown, much smaller than the succeeding premaxillary teeth, and never reaches the height of the highest maxillary tooth. Another notable feature is that the first premaxillary tooth of *Bagualosaurus agudoensis* is caudally retreated, leaving an edentulous rostral portion on the upper jaw. Among the sauropodomorphs sampled for the phylogenetic analysis, this seems to be shared only with some specimens of *P. engelhardti* (Galton, 1984; Yates, 2003a; Prieto-Márquez & Norell, 2011), but this characteristic is also present in the ornithischians *Lesothosaurus diagnosticus* and *Heterodontosaurus tucki* (Sereno, 1991, 2012; Norman *et al.*, 2011), in which the premaxilla is interpreted to be covered by a keratinous ramphotheca. Indeed, the presence of a ramphotheca has already been proposed for *P. engelhardti* (Sereno, 1997, 2007) based on the presence of a great concentration of foramina and/or parasagittal ridges along the rostral portion of the premaxilla, as also seen in *Riojasaurus incertus*, *Adeopapposaurus mognai* and *Mussaurus patagonicus* (Bonaparte & Pluameres, 1995; Pol & Powell, 2007; Martínez, 2009). Several foramina are also reported along the tooth row of *M. carinatus* (Sues *et al.*, 2004), but the authors reject the hypothesis of a beak for the taxon, given the proximity of the first premaxillary tooth and the rostral margin of the premaxilla. Although the premaxillary teeth of *B. agudoensis* are retracted from the rostralmost portion of the premaxilla, resembling the condition of some specimens of *P. engelhardti* (Galton, 1984; Prieto-Márquez & Norell, 2011), the absence of ridges or additional foramina in the premaxillary body implies the absence of a ramphotheca in the taxon. Indeed, as discussed by Yates (2003b), the morphology of this region varies among sauropodomorphs, and the putative presence of a premaxillary beak is still controversial. In any case, other Carnian sauropodomorphs lack retracted premaxillary teeth (Cabreira *et al.*, 2011, 2016; Sereno *et al.*, 2013), suggesting that they belong to earlier divergences relative to *B. agudoensis*.

Another feature of the skull of *Bagualosaurus agudoensis* that approaches the condition of post-Carnian sauropodomorphs, differing from that of coeval forms, is the relatively straight and continuous alveolar margin at the premaxilla–maxilla articulation. Although not all early sauropodomorphs show a subnarial gap, at least a diastema is present between the premaxillary and maxillary tooth

rows of *Eoraptor lunensis*, *Pampadromaeus barberenai* and *Buriolestes schultzi* (Cabreira *et al.*, 2011, 2016; Sereno *et al.*, 2013). Such diastemas seem to be related to the opening of the subnarial foramen, which is located close to the alveolar margin. This is clear in the holotypes of *E. lunensis* and *Bu. schultzi*, in which the subnarial foramen perforates the rostral tip of the cranial process of the maxilla, and is directed rostroventrally towards the tooth gap. In *Ba. agudoensis*, the subnarial opening is positioned more dorsally distant from the alveolar margin. Additionally, its rim is marked by notches in both the premaxilla and the maxilla. In post-Carnian sauropodomorphs, the subnarial foramen is located even more dorsally (Yates, 2003a, 2007; Sues *et al.*, 2004; Martínez, 2009; Prieto-Márquez & Norell, 2011), and as in *Ba. Agudoensis*, both the premaxilla and the maxilla contribute to its margins.

Despite the above discussed features, several characteristics of the skull of *Bagualosaurus agudoensis* are reminiscent of earlier forms. The rostral process of the maxilla is sloped as in *Eoraptor lunensis*, *Pampadromaeus barberenai* and *Buriolestes schultzi*, rather than assuming the typical subquadrangular shape seen in post-Carnian forms like *Plateosaurus engelhardti*, *Adeopapposaurus mognai*, *Coloradisaurus brevis* and *Massospondylus carinatus* (Galton, 1984; Sues *et al.*, 2004; Martínez, 2009; Apaldetti *et al.*, 2014). *Ba. agudoensis* also has a marked longitudinal ridge that extends parallel to the ventral margin of the maxillary portion of the antorbital fossa. This is seen in all Carnian sauropodomorphs with a preserved maxilla (*Eo. lunensis*, *Pa. barberenai* and *Bu. schultzi*), but not in most post-Carnian taxa (Galton, 1984; Bonaparte & Pluameres, 1995; Yates, 2003b, 2007; Martínez, 2009; Apaldetti *et al.*, 2014). Additionally, the ventral portion of the antorbital fossa of *Ba. agudoensis* extends along the entire dorsal margin of the caudal process of the maxilla, resembling *E. lunensis*, whereas in post-Carnian taxa (e.g. *Pl. engelhardti*, *Efraasia minor* and *Riojasaurus incertus*) the fossa only extends up to the midpoint of that process, as also likely reported for *Pa. barberenai* (Galton, 1984; Bonaparte & Pluameres, 1995; Yates, 2003a; Cabreira *et al.*, 2011). Furthermore, *Ba. agudoensis* has a longitudinal groove in the dorsal surface of the ventral margin of the antorbital fossa that resembles the neurovascular sulcus recognized by Witmer (1997) for *Pl. engelhardti* and other sauropodomorphs, which is apparently absent in early forms like *Eo. lunensis* and *Pa. barberenai*. By contrast, the jugal of *Ba. agudoensis* is excluded from the antorbital fossa, differing from the condition seen in post-Carnian taxa. This is achieved partly due to the development of the antorbital fossa at the ventral ramus of the lacrimal, as is also seen in *Eo. lunensis* (Sereno *et al.*, 2013). *Pantyraco caducus* also shows a wide contribution of

the lacrimal to the caudoventral portion of the antorbital fossa (Yates, 2003b; Galton & Kermack, 2010), resembling *Ba. agudoensis* and *Eo. lunensis*, but it is not clear if this structure excluded the jugal from the antorbital fenestra.

The lower jaw of *Bagualosaurus agudoensis* also shows typical sauropodomorph features, like the edentulous, ventrally sloped rostral tip and the probable ventrally displaced articulation. The dentary of *Bagualosaurus agudoensis* is relatively high relative to its length, a feature that resembles more the condition of taxa like *Pantyraco caducus*, *Plateosaurus engelhardti* and *Efraasia minor* (Galton, 1984; Benton *et al.*, 2000; Yates, 2003a, b; Galton & Kermack, 2010), than of coeval early sauropodomorphs, which have a relatively lower and longer dentary. Additionally, as in post-Carnian taxa, the caudoventral process of the dentary of *B. agudoensis* may be shorter than the caudodorsal. The caudoventral process of *Eoraptor lunensis*, *Panphagia protos* and *Pampadromaeus barberenai* has been interpreted as longer, but this condition is somewhat ambiguous in the holotypes of *Eo. lunensis* (Sereno *et al.*, 2013) and *B. agudoensis*.

Differing from post-Carnian sauropodomorphs, the dentary of *Bagualosaurus agudoensis* does not possess a buccal emargination, with the tooth row placed at the same level of the lateral margin of the dentary. Additionally, *B. agudoensis* shares with *Panphagia protos* a prominent shelf in the surangular (Martínez & Alcober, 2009), absent in other sauropodomorphs.

In contrast to the skull and mandible, the postcranial skeleton of *Bagualosaurus agudoensis* resembles more that of early sauropodomorphs, sharing few anatomical features with post-Carnian taxa. The relative length of the ilium resembles that of other early dinosaurs like *Eoraptor lunensis*, *Saturnalia tupiniquim* and *Herrerasaurus ischigualastensis* (Novas, 1993; Langer, 2003; Sereno *et al.*, 2013). Also, the straight ventral margin of the iliac acetabulum is similar to that of other early sauropodomorphs (Langer, 2003; Martínez & Alcober, 2009; Ezcurra, 2010; Sereno *et al.*, 2013; Cabreira *et al.*, 2016). On the contrary, post-Carnian sauropodomorphs have a distinctly concave ventral margin on the iliac acetabular wall (von Huene, 1926; Galton, 1973; Cooper, 1981; Yates, 2003b; Martínez, 2009). The position of the widest portion of the supracetabular crest also resembles that of early sauropodomorphs, located at the midpoint of the acetabulum (Yates, 2003b). The laterally flared supracetabular crest, as well as the flat roof of the iliac acetabulum, are rather unique among sauropodomorphs, with only one potential analogue (Mcphee & Choiniere, 2016). Among sauropodomorphs, the pubis of *B. agudoensis* is reminiscent of that of early forms like *E. lunensis* and *S. tupiniquim* (Langer, 2003; Sereno *et al.*, 2013), given the presence of a marked pubic tubercle,

a structure lost in post-Carnian forms like *Efraasia minor*, *Plateosaurus engelhardti* and *Massospondylus carinatus* (von Huene, 1926; Galton, 1973; Cooper, 1981). Additionally, the pubic tubercle of *B. agudoensis* is remarkable by the presence of a longitudinal sulcus, not seen in any other of the compared taxa. This is here interpreted as an autapomorphic feature of the taxon, also seen in another dinosaur specimen from the Janner site, UFRGS-PV-1240-T (Pretto et al., 2015), suggesting that it might represent a second specimen of *B. agudoensis*, even larger than the holotype.

The craniomedially set femoral head of *Bagualosaurus agudoensis* represents a plesiomorphic feature present in most early dinosaurs (Carrano, 2000; Hutchinson, 2001b). The same is true for the sigmoid shape of the bone, which is widespread among early dinosaurs (Novas, 1993; Langer, 2003; Cabreira et al., 2011, 2016; Martínez et al., 2011; Sereno et al., 2013). The slightly faint trochanteric shelf and cranial trochanter of *Ba. agudoensis* are somewhat distinct from coeval sauropodomorphs (e.g. *Eoraptor lunensis*, *Saturnalia tupiniquim*, *Pampadromaeus barberenai* and *Buriolestes schultzi*). However, the presence of a trochanteric shelf, despite its faintness, allows *B. agudoensis* to be distinguished from post-Carnian sauropodomorphs, as well as *Guaibasaurus candelariensis*. Indeed, these structures become progressively less developed in later sauropodomorphs, like *Plateosaurus engelhardti*, *Efraasia minor*, *Adeopapposaurus mognai* and *Massospondylus carinatus* (von Huene, 1926; Galton, 1973; Cooper, 1981; Martínez, 2009), as well as *G. candelariensis* (Langer et al., 2011), but were also suggested to be highly dependent on ontogeny and possibly sexual dimorphism (Nesbitt et al., 2009; Piechowski et al., 2014). The surface that received the insertion of m. caudofemoralis longus is also subject to some variation among early sauropodomorphs. The slight bump cranial to the fourth trochanter of *Ba. agudoensis* is similar to the strong rugosity observed in *Bu. schultzi*, *Pa. barberenai* and *Eo. lunensis* (PVSJ 559). In *S. tupiniquim* and *Chromogisaurus novasi*, by contrast, the insertion area of the m. caudofemoralis longus is marked by a well-defined oval fossa (Langer, 2003; Ezcurra, 2010). In post-Carnian sauropodomorphs (e.g. *A. mognai*, *Pl. engelhardti* and *Ef. minor*), there is no marked concavity, nor a conspicuous raised bump or muscular scar, although the muscular attachment is indicated in some specimens by a different texture on the bone.

The fibular articular facet on the lateral tibia is slightly scarred in *Bagualosaurus agudoensis*, resembling the condition in *Panphagia protos*, but not other coeval sauropodomorphs. In *Eoraptor lunensis*, *Chromogisaurus novasi* and *Saturnalia tupiniquim*, this area is marked by a strong rugosity (Langer, 2003; Ezcurra, 2010; Sereno et al., 2013), which may also occur in *Buriolestes schultzi*.

This seems to be one of the few postcranial features shared by *Ba. agudoensis* and post-Carnian sauropodomorphs, including *Pantydraco caducus*, *Efraasia minor*, *Plateosaurus engelhardti* and *Adeopapposaurus mognai* (von Huene, 1926; Galton, 1976; Yates, 2003b; Galton, Yates & Kermack, 2007; Martínez, 2009; Galton & Kermack, 2010). On the contrary, the subquadrangular distal tibia is reminiscent of the condition in coeval early sauropodomorphs and other early dinosaurs (e.g. *Herrerasaurus ischigualastensis*). In Norian sauropodomorphs, like *Pa. caducus*, *Ef. minor* and *Pl. engelhardti*, the distal tibia is lateromedially expanded, assuming a subrectangular shape.

The most distinctive feature of the distal tibia of *Bagualosaurus agudoensis* is, however, its well-marked caudomedial notch. This feature is absent in all early sauropodomorphs, and strongly resembles the condition shown by *Zupaysaurus rougieri* (Ezcurra & Novas, 2007), also widespread among neotheropods and present in *Guaibasaurus candelariensis* (Langer et al., 2011). The presence of the caudomedial notch in the distal tibia of *B. agudoensis* indicates that the distribution of this character is more complex than previously thought. Indeed, the possibility that *G. candelariensis* corresponds to an early saurischian (Cabreira et al., 2016) rather than a theropod, as previously suggested (Langer et al., 2011), might indicate that this character is plesiomorphic in the group.

The pes of *Bagualosaurus agudoensis* is gracile, differing from the robust construction of larger forms, like *Plateosaurus engelhardti* (von Huene, 1926; Galton, 1976). The marked extensor depressions in most metatarsals and phalanges resemble those of early sauropodomorphs like *Eoraptor lunensis*, *Buriolestes schultzi* and *Saturnalia tupiniquim* (Langer, 2003; Sereno et al., 2013; Cabreira et al., 2016). These are not evident in post-Carnian forms like *Pantydraco caducus*, *Efraasia minor* and *Pl. engelhardti*, or occur as slight scars, as in *Adeopapposaurus mognai* (von Huene, 1926; Galton, 1973; Yates, 2003b; Martínez, 2009; Galton & Kermack, 2010).

CONCLUSION

Bagualosaurus agudoensis represents the largest known Carnian sauropodomorph. Indeed, if the material described by Pretto et al. (2015) is regarded as a second specimen of the taxon, its body size would rival that of many other Carnian taxa (e.g. rhynchosaurs and cynodonts, at least from Brazilian faunas). Despite that, *B. agudoensis* is far from achieving the large body sizes of most post-Carnian sauropodomorphs. Indeed, most traits related to large body masses (such as robust

hindlimbs, especially the pes) are not yet present in *B. agudoensis*, and most traits shared with post-Carnian sauropodomorphs seem to be related to the skull and mandible. This suggests that modification in the skull anatomy, possibly related to more efficient herbivorous habits, appeared earlier in the evolution of sauropodomorphs than their further increase in size.

The discovery of *Bagualosaurus agudoensis* adds to the known dinosaur diversity of the Carnian. It also reinforces the idea that sauropodomorphs had an initial moment of high diversification, prior to their increase in abundance achieved during the Norian and afterwards when the group started to represent a dominant component of many paleoenvironments (Brusatte *et al.*, 2010; Ezcurra, 2010; Langer *et al.*, 2010; Irmis, 2011).

ACKNOWLEDGEMENTS

The authors express their gratitude to Dr Téo V. de Oliveira and Dr Cristina Bertoni-Machado, who provided details of the collection and early preparation of UFRGS-PV-1099-T, to Luís F. Lopes, for the photographic work on UFRGS-PV-1099-T and to Dr Jonathan S. Bittencourt, who kindly provided photographs of specimens for comparison. Dr Bianca M. Mastrantonio, Dr Felipe L. Pinheiro, Dr Marco B. de Andrade, Dr Leonardo Kerber and Rodrigo T. Müller provided helpful comments on early versions of this manuscript. The authors express their gratitude to the reviewers, Dr Peter M. Galton and Dr Matthew G. Baron. This study was partially funded by grants provided by Conselho Nacional de Desenvolvimento Científico e Tecnológico (CNPq) to FAP (process 140743/2012-0) and Fundação de Amparo à Pesquisa do Estado de São Paulo (FAPESP) to MCL (process number 2014/03825-3). Thanks are also given to the Willi Henning Society, for the gratuity of TNT software.

REFERENCES

- Abdala F, Ribeiro AM, Schultz CL. 2001.** A rich cynodont fauna of Santa Cruz do Sul, Santa Maria Formation (middle-late Triassic), Southern Brazil. *Neues Jahrbuch für Geologie und Paläontologie, Monatshefte*: 669–687. <https://onlinelibrary.wiley.com/doi/abs/10.1111/j.1096-3642.2003.00096.x>
- Apaldetti C, Martinez RN, Pol D, Souter T. 2014.** Redescription of the skull of *Coloradisaurus brevis* (Dinosauria, Sauropodomorpha) from the late Triassic Los Colorados Formation of the Ischigualasto-Villa Union Basin, Northwestern Argentina. *Journal of Vertebrate Paleontology* **34**: 1113–1132.
- Baron MG, Norman DB, Barrett PM. 2017a.** A new hypothesis of dinosaur relationships and early dinosaur evolution. *Nature* **543**: 501–506.
- Baron MG, Norman DB, Barrett PM. 2017b.** Baron *et al.* reply. *Nature* **551**: E4–E5.
- Behrensmeyer AK. 1978.** Taphonomic and ecologic information from bone weathering. *Paleobiology* **4**: 150–162.
- Benton MJ, Juul L, Storrs G, Galton PM. 2000.** Anatomy and systematics of the prosauropod dinosaur *Thecodontosaurus antiquus* from the Upper Triassic of southwest England. *Journal of Vertebrate Paleontology* **20**: 77–108.
- Bonaparte JF, Plumas JA. 1995.** Notas sobre el primer craneo de *Riojasaurus incertus* (Dinosauria, Prosauropoda, Melanorosauridae) del Triasico Superior de La Rioja, Argentina. *Ameghiniana* **32**: 341–349.
- Brusatte SL, Nesbitt SJ, Irmis RB, Butler RJ, Benton MJ, Norell MA. 2010.** The origin and early radiation of dinosaurs. *Earth-Science Reviews* **101**: 68–100.
- Cabreira SF, Schultz CL, de Bittencourt JS, Soares MB, Fortier DC, Silva LR, Langer MC. 2011.** New stem-sauropodomorph (Dinosauria, Saurischia) from the Triassic of Brazil. *Naturwissenschaften* **98**: 1035–1040.
- Cabreira SF, Kellner AWA, Dias-da-Silva S, Silva LR, Bronzati M, de Marsola JCA, Müller RT, de Bittencourt JS, Batista BJ, Raugust T, Carrilho R, Brodt A, Langer MC. 2016.** A unique late Triassic dinosauromorph assemblage reveals dinosaur ancestral anatomy and diet. *Current Biology* **26**: 3090–3095.
- Cabrera A. 1943.** El primer hallazgo de terápsidos en la Argentina. *Notas del Museo de La Plata, Paleontología* **8**: 317–331.
- Cambra-Moo O, Buscalioni AD. 2003.** Biostratigraphic patterns in archosaur fossils: influence of morphological organization on dispersal. *Journal of Taphonomy* **1**: 247–268.
- Carrano MT. 2000.** Homoplasy and the evolution of dinosaur locomotion. *Paleobiology* **26**: 489–512.
- Cooper MR. 1981.** The prosauropod dinosaur *Massospondylus carinatus* Owen from Zimbabwe: Its biology, mode of life and phylogenetic significance. *Occasional Papers of the National Museum Mon. Rhodesia B* **6**: 689–840.
- Ezcurra MD. 2010.** A new early dinosaur (Saurischia: Sauropodomorpha) from the late Triassic of Argentina: a reassessment of dinosaur origin and phylogeny. *Journal of Systematic Palaeontology* **8**: 371–425.
- Ezcurra MD, Apaldetti C. 2012.** A robust sauropodomorph specimen from the Upper Triassic of Argentina and insights on the diversity of the Los Colorados Formation. *Proceedings of the Geologists' Association* **123**: 155–164.
- Ezcurra MD, Novas FE. 2007.** Phylogenetic relationships of the Triassic theropod *Zupaysaurus rougieri* from NW Argentina. *Historical Biology* **19**: 35–72.
- Galton PM. 1973.** On the anatomy and relationships of *Efraasia diagnostica* (Huene) n. gen., a prosauropod dinosaur (Reptilia: Saurischia) from the Upper Triassic of Germany. *Paläontologische Zeitschrift* **47**: 229–255.
- Galton PM. 1976.** Prosauropod dinosaurs (Reptilia: Saurischia) of North America. *Postilla* **169**: 1–98.
- Galton PM. 1984.** Cranial anatomy of the prosauropod dinosaur *Plateosaurus* from the Knollenmergel (Middle Keuper, Upper Triassic) of Germany. I. Two complete skulls from Trossingen/Württemberg, with comments on the diet. *Geologica et Palaeontologica* **18**: 139–171.

- Galton PM. 1985.** Cranial anatomy of the prosauropod dinosaur *Plateosaurus* from the Knollenmergel (Middle Keuper, Upper Triassic) of Germany. II. All the cranial material and details of soft-part anatomy. *Geologica et Palaeontologica* **19**: 119–159.
- Galton PM, Kermack D. 2010.** The anatomy of *Pantyraco caducus*, a very basal sauropodomorph dinosaur from the Rhaetian (Upper Triassic) of South Wales UK. *Revue de Paleobiologie* **29**: 341–404.
- Galton PM, Yates AM, Kermack D. 2007.** *Pantyraco* n. gen. for *Thecodontosaurus caducus* Yates, 2003, a basal sauropodomorph dinosaur from the Upper Triassic or Lower Jurassic of South Wales, UK. *Neues Jahrbuch für Geologie und Paläontologie—Abhandlungen* **243**: 119–125.
- Gauthier J. 1986.** Saurischian Monophyly and the Origin of Birds. In K. Padian, ed. *The Origin of Birds and the Evolution of Flight. Memoir of the California Academy of Science* **8**: 1–55.
- Goloboff PA. 2014.** Extended implied weighting. *Cladistics* **30**: 260–272.
- Goloboff PA, Catalano SA. 2016.** TNT version 1.5, including a full implementation of phylogenetic morphometrics. *Cladistics* **32**: 221–238.
- Goloboff PA, Carpenter JM, Arias JS, Esquivel DRM. 2008a.** Weighting against homoplasy improves phylogenetic analysis of morphological data sets. *Cladistics* **24**: 758–773.
- Goloboff PA, Farris JS, Nixon KC. 2008b.** TNT, a free program for phylogenetic analysis. *Cladistics* **24**: 774–786.
- Goloboff PA, Torres A, Arias JS.** In press. Weighted parsimony outperforms other methods of phylogenetic inference under models appropriate for morphology. *Cladistics*: 1–31.
- Holz M, Schultz CL. 1998.** Taphonomy of the south Brazilian Triassic herpetofauna: fossilization mode and implications for morphological studies. *Lethaia* **31**: 335–345.
- Horn BLD, Melo TM, Schultz CL, Philipp RP, Kloss HP, Goldberg K. 2014.** A new third-order sequence stratigraphic framework applied to the Triassic of the Paraná Basin, Rio Grande do Sul, Brazil, based on structural, stratigraphic and paleontological data. *Journal of South American Earth Sciences* **55**: 123–132.
- von Huene F. 1926.** Vollständige Osteologie eines Plateosauriden aus dem schwäbischen Keuper. *Geologie und Paläontologie Abhandlungen, Neue Folge* **15**: 139–179.
- Hutchinson J. 2001a.** The evolution of pelvic osteology and soft tissues on the line to extant birds (Neornithes). *Zoological Journal of the Linnean Society* **131**: 123–168.
- Hutchinson J. 2001b.** The evolution of femoral osteology and soft tissues on the line to extant birds (Neornithes). *Zoological Journal of the Linnean Society* **131**: 169–197.
- Irmis RB. 2011.** Evaluating hypotheses for the early diversification of dinosaurs. *Earth and Environmental Science Transactions of the Royal Society of Edinburgh* **101**: 397–426.
- Langer MC. 2003.** The pelvic and hind limb anatomy of the stem-sauropodomorph *Saturnalia tupiniquim* (late Triassic, Brazil). *PaleoBios* **23**: 1–40.
- Langer MC. 2005.** Studies on continental late Triassic tetrapod biochronology. II. The Ischigualastian and a Carnian global correlation. *Journal of South American Earth Sciences* **19**: 219–239.
- Langer MC. 2014.** The origins of Dinosauria: much ado about nothing. *Palaeontology* **57**: 469–478.
- Langer MC, Abdala F, Richter M, Benton MJ. 1999.** A sauropodomorph dinosaur from the Upper Triassic (Carnian) of southern Brazil. *Comptes Rendus de l'Academie des Sciences, Paris* **329**: 511–517.
- Langer MC, Ezcurra MD, de Bittencourt JS, Novas FE. 2010.** The origin and early evolution of dinosaurs. *Biological Reviews of the Cambridge Philosophical Society* **85**: 55–110.
- Langer MC, de Bittencourt J S, Schultz CL. 2011.** A reassessment of the basal dinosaur *Guaibasaurus candelariensis*, from the late Triassic Caturrita Formation of south Brazil. *Earth and Environmental Science Transactions of the Royal Society of Edinburgh* **101**: 301–332.
- Langer MC, Ezcurra MD, Rauhut OWM, Benton MJ, Knoll F, McPhee BW, Novas FE, Pol D, Brusatte SL. 2017.** Untangling the dinosaur family tree. *Nature* **551**: E1–E3.
- Langer MC, Ramezani J, Da Rosa ÁAS. 2018.** U-Pb age constraints on dinosaur rise from south Brazil. *Gondwana Research* **57**: 133–140.
- Legg DA, Sutton MD, Edgecombe GD. 2013.** Arthropod fossil data increase congruence of morphological and molecular phylogenies. *Nature Communications* **4**: 1–7.
- Liparini A, Oliveira TV, Pretto FA, Soares MB, Schultz CL. 2013.** The lower jaw and dentition of the traversodontid *Exaeretodon riograndensis* Abdala, Barberena & Dornelles, from the Brazilian Triassic (Santa Maria 2 Sequence, Hyperodapedon Assemblage Zone). *Alcheringa: an Australasian Journal of Palaeontology* **37**: 1–7.
- Martínez RN. 2009.** *Adeopapposaurus mognai*, gen. et sp. nov. (Dinosauria: Sauropodomorpha), with comments on adaptations of basal Sauropodomorpha. *Journal of Vertebrate Paleontology* **29**: 142–164.
- Martínez RN, Alcober OA. 2009.** A basal Sauropodomorph (Dinosauria: Saurischia) from the Ischigualasto formation (Triassic, Carnian) and the early evolution of Sauropodomorpha. *PLoS ONE* **4**: e4397.
- Martínez RN, Sereno PC, Alcober OA, Colombi CE, Renne PR, Montañez IP, Currie BS. 2011.** A basal dinosaur from the dawn of the dinosaur era in southwestern Pangaea. *Science* **331**: 206–210.
- Martínez RN, Apaldetti C, Abelin D. 2012.** Basal sauropodomorphs from the Ischigualasto formation. *Journal of Vertebrate Paleontology* **32**: 51–69.
- Martínez RN, Apaldetti C, Alcober OA, Colombi CE, Sereno PC, Fernandez E, Malnis PS, Correa GA, Abelin D. 2013.** Vertebrate succession in the Ischigualasto Formation. *Journal of Vertebrate Paleontology* **32**: 10–30.
- McPhee BW, Choiniere JN. 2016.** A hyper-robust sauropodomorph dinosaur ilium from the Upper Triassic–Lower Jurassic Elliot Formation of South Africa: implications for the functional diversity of basal Sauropodomorpha. *Journal of African Earth Sciences* **123**: 177–184.
- Müller R, Langer MC, Aires A, Dias-da-Silva S. 2014.** New dinosauriform (Ornithodira, Dinosauromorpha) record from the late Triassic of Southern Brazil. *Paleontological Research* **18**: 118–121.
- Nesbitt SJ. 2011.** The early evolution of archosaurs : relationships and the origin of major clades. *Bulletin of the American Museum of Natural History*: 1–292.

- Nesbitt SJ, Irmis RB, Parker WG, Smith ND, Turner AH, Rowe T. 2009. Hindlimb osteology and distribution of basal dinosauromorphs from the late Triassic of North America. *Journal of Vertebrate Paleontology* **29**: 498–516.
- Norman DB, Crompton AW, Butler RJ, Porro LB, Charig AJ. 2011. The Lower Jurassic ornithischian dinosaur *Heterodontosaurus tucki* Crompton & Charig, 1962: cranial anatomy, functional morphology, taxonomy, and relationships. *Zoological Journal of the Linnean Society* **163**: 182–276.
- Novas FE. 1993. New information on the systematics and postcranial skeleton of *Herrerasaurus ischigualastensis* (Theropoda: Herrerasauridae) from the Ischigualasto formation (Upper Triassic) of Argentina. *Journal of Vertebrate Paleontology* **13**: 400–423.
- Novas FE, Ezcurra MD, Chatterjee S, Kuttu TS. 2011. New dinosaur species from the Upper Triassic Upper Maleri and Lower Dharmaram formations of Central India. *Earth and Environmental Science Transactions of the Royal Society of Edinburgh* **101**: 333–349.
- de Oliveira TV, Schultz CL, Soares MB. 2007. O esqueleto pós-craniano de *Exaeretodon riograndensis* Abdala et al. (Cynodontia, Traversodontidae), Triássico do Brasil. *Revista Brasileira de Paleontologia* **10**: 79–94.
- de Oliveira TV, Soares MB, Schultz CL. 2010. *Trucidocynodon riograndensis* gen. nov. et sp. nov. (Eucynodontia), a new cynodont from the Brazilian Upper Triassic (Santa Maria Formation). *Zootaxa* **2382**: 1–71.
- Padian K, & May C.L. 1993. The earliest dinosaurs. *New Mexico Museum of Natural History & Science Bulletin* **3**: 379–381.
- Paes Neto VD, Parkinson AH, Pretto FA, Soares MB, Schwanke C, Schultz CL, Kellner AW. 2016. Oldest evidence of osteophagic behavior by insects from the Triassic of Brazil. *Palaeogeography, Palaeoclimatology, Palaeoecology* **453**: 30–41.
- Piechowski R, Tałanda M, Dzik J. 2014. Skeletal variation and ontogeny of the late Triassic dinosauriform *Silesaurus opolensis*. *Journal of Vertebrate Paleontology* **34**: 1383–1393.
- Pol D, Powell JE. 2007. Skull anatomy of *Mussaurus patagonicus* (Dinosauria: Sauropodomorpha) from the late Triassic of Patagonia. *Historical Biology* **19**: 125–144.
- Pretto FA, Schultz CL, Langer MC. 2015. New dinosaur remains from the late Triassic of southern Brazil (Candelária Sequence, Hyperodapedon Assemblage Zone). *Alcheringa: an Australasian Journal of Palaeontology* **39**: 264–273.
- Prieto-Márquez A, Norell MA. 2011. Redescription of a nearly complete skull of *Plateosaurus* (Dinosauria: Sauropodomorpha) from the late Triassic of Trossingen (Germany). *American Museum Novitates*: 1–58.
- Rogers RR, Swisher III CC, Sereno PC, Monetta AM, Forster CA, Martínez RN. 1993. The ischigualasto tetrapod assemblage (late Triassic, Argentina) and 40Ar/39Ar dating of dinosaur origins. *Science* **260**: 794–797.
- Sander PM, Clauss M. 2008. Sauropod gigantism. *Science* **322**: 200–201.
- Sander PM, Christian A, Clauss M, Fechner R, Gee CT, Griebeler EM, Gunga HC, Hummel J, Mallison H, Perry SF, Preuschoft H, Rauhut OWM, Remes K, Tütken T, Wings O, Witzel U. 2011. Biology of the sauropod dinosaurs: the evolution of gigantism. *Biological Reviews of the Cambridge Philosophical Society* **86**: 117–55.
- Sereno P. 1991. *Lesothosaurus*, ‘Fabrosaurids’, and the early evolution of Ornithischia. *Journal of Vertebrate Paleontology* **11**: 168–197.
- Sereno PC. 1997. The origin and evolution of dinosaurs. *Annual Reviews of Earth and Planetary Sciences* **25**: 435–489.
- Sereno PC. 2007. The phylogenetic relationships of early dinosaurs: a comparative report. *Historical Biology* **19**: 145–155.
- Sereno PC. 2012. Taxonomy, morphology, masticatory function and phylogeny of heterodontosaurid dinosaurs. *ZooKeys* **226**: 1–225.
- Sereno PC, Forster CA, Rogers RR, Monetta AM. 1993. Primitive dinosaur skeleton from Argentina and the early evolution of the Dinosauria. *Nature* **361**: 64–66.
- Sereno PC, Martínez RN, Alcober OA. 2013. Osteology of *Eoraptor lunensis* (Dinosauria, Sauropodomorpha). *Journal of Vertebrate Paleontology* **32**: 83–179.
- Smith ND, Pol D. 2007. Anatomy of a basal sauropodomorph dinosaur from the early Jurassic Hanson Formation of Antarctica. *Acta Palaeontologica Polonica* **52**: 657–674.
- Sues HD, Reisz RR, Hinic S, Raath MA. 2004. On the skull of *Massospondylus carinatus* Owen, 1854 (Dinosauria: Sauropodomorpha) from the Elliot and Clarens formations (Lower Jurassic) of South Africa. *Annals of Carnegie Museum* **73**: 239–257.
- Wedel M. 2007. What pneumaticity tells us about ‘prosauropods’, and vice versa. *Special Papers in Palaeontology* **77**: 207–222.
- Wilson JA. 1999. A nomenclature for vertebral laminae in sauropods and other saurischian dinosaurs. *Journal of Vertebrate Paleontology* **19**: 639–653.
- Witmer LM. 1997. The evolution of the antorbital cavity of archosaurs: a study in soft-tissue reconstruction in the fossil record with an analysis of the function of pneumaticity. *Journal of Vertebrate Paleontology* **17**: 1–76.
- Yates AM. 2003a. The species taxonomy of the sauropodomorph dinosaurs from the Löwenstein Formation (Norian, late Triassic) of Germany. *Palaeontology* **46**: 317–337.
- Yates AM. 2003b. A new species of the primitive dinosaur *Thecodontosaurus* (Saurischia: Sauropodomorpha) and its implications for the systematics of early dinosaurs. *Journal of Systematic Palaeontology* **1**: 1–42.
- Yates AM. 2007. The first complete skull of the Triassic dinosaur *Melanorosaurus* Houghton (Sauropodomorpha: Anchisauria). *Special Papers in Palaeontology* **77**: 9–55.

SUPPORTING INFORMATION

Additional Supporting Information may be found in the online version of this article at the publisher’s web-site.